

AD-A136 775

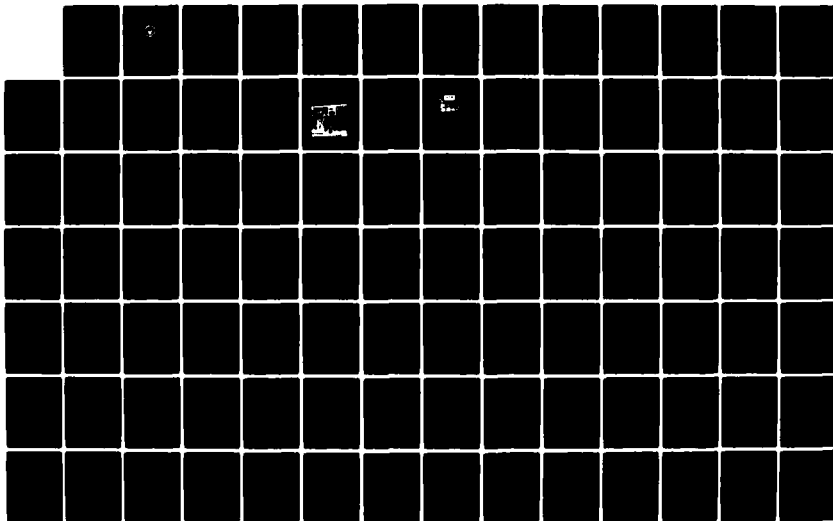
AN ERROR ANALYSIS OF RANGE-AZIMUTH POSITIONING(U) NAVAL  
POSTGRADUATE SCHOOL MONTEREY CA D A WALTZ SEP 83

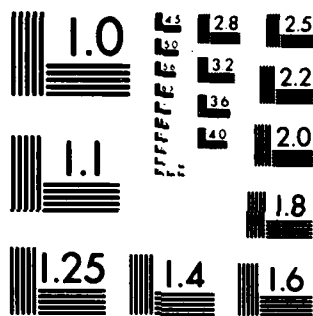
1/2

UNCLASSIFIED

F/G 8/2

NL





MICROCOPY RESOLUTION TEST CHART  
NATIONAL BUREAU OF STANDARDS 1963-A

A136775

NAVAL POSTGRADUATE SCHOOL  
Monterey, California



THESIS

DTIC  
COLLECTED  
JAN 13 1984  
A

AN ERROR ANALYSIS OF  
RANGE-AZIMUTH POSITIONING

by

David A. Waltz

September 1983

Thesis Advisor:

G. B. Mills

Approved for public release; distribution unlimited

DTIC FILE COPY

84 01 15 011

UNCLASSIFIED

SECURITY CLASSIFICATION OF THIS PAGE (When Data Entered)

REPORT DOCUMENTATION PAGE		READ INSTRUCTIONS BEFORE COMPLETING FORM
1. REPORT NUMBER	2. GOVT ACCESSION NO. AD-A136775	3. RECIPIENT'S CATALOG NUMBER
4. TITLE (and Subtitle) AN ERROR ANALYSIS OF RANGE-AZIMUTH POSITIONING		5. TYPE OF REPORT & PERIOD COVERED Master's Thesis September, 1983
		6. PERFORMING ORG. REPORT NUMBER
7. AUTHOR(s)  David A. Waltz		8. CONTRACT OR GRANT NUMBER(s)
9. PERFORMING ORGANIZATION NAME AND ADDRESS Naval Postgraduate School Monterey, California 93943		10. PROGRAM ELEMENT, PROJECT, TASK AREA & WORK UNIT NUMBERS
11. CONTROLLING OFFICE NAME AND ADDRESS Naval Postgraduate School Monterey, California 93943		12. REPORT DATE September, 1983
		13. NUMBER OF PAGES 103
14. MONITORING AGENCY NAME & ADDRESS (if different from Controlling Office)		15. SECURITY CLASS. (of this report) Unclassified
		15a. DECLASSIFICATION/DOWNGRADING SCHEDULE
16. DISTRIBUTION STATEMENT (of this Report) Approved for public release; distribution unlimited		
17. DISTRIBUTION STATEMENT (of the abstract entered in Block 20, if different from Report)		
18. SUPPLEMENTARY NOTES		
19. KEY WORDS (Continue on reverse side if necessary and identify by block number) Hydrography, surveying, range-azimuth, theodolites, hydrographic surveying		
20. ABSTRACT (Continue on reverse side if necessary and identify by block number)  Pointing error standard deviations for two theodolites, the Wild T-2 and Odom Aztrac, were determined under conditions closely approximating those of range-azimuth or azimuth-azimuth hydrographic surveys. Pointing errors found for both instruments were about 1.3 meters, and were independent of distance. No statistical difference between the errors of the two instruments was found. The accuracy of the interpolation methods used by the National Ocean Service (NOS) for range-azimuth positioning were investigated, and an average inverse		

DD FORM 1 JAN 79 1473

EDITION OF 1 NOV 66 IS OBSOLETE  
5/N 0102-LP-014-6601

1

UNCLASSIFIED

SECURITY CLASSIFICATION OF THIS PAGE (When Data Entered)

UNCLASSIFIED

SECURITY CLASSIFICATION OF THIS PAGE (When Data Entered)

block 20 continued:

distance of about 2.5 meters was observed between interpolated positions and corresponding observed positions. The overall range-azimuth position errors of the two theodolites were then compared to positioning standards of NOS and the International Hydrographic Organization, using assumed ranging standard deviations of 1.0 and 3.0 meters. Both instruments met all standards except the NOS range-azimuth standard for 1:5,000 scale surveys. Interpolated positions may fail to meet more of the standards because of additional inherent error.



Accession For	
NTIS GRA&I	<input checked="" type="checkbox"/>
DTIC TAB	<input type="checkbox"/>
Unannounced	<input type="checkbox"/>
Justification	
Distribution/	
Availability Codes	
Avail and/or	
Special	
A1	

S. N 0102- LF 014-6601

UNCLASSIFIED

SECURITY CLASSIFICATION OF THIS PAGE(When Data Entered)

Approved for public release; distribution unlimited.

An Error Analysis  
of  
Range-Azimuth Positioning

by

David A. Waltz  
Lieutenant, National Oceanic and Atmospheric Administration  
B.S., University of Alabama, 1971

Submitted in partial fulfillment of the  
requirements for the degree of

MASTER OF SCIENCE IN OCEANOGRAPHY (HYDROGRAPHY)

from the

NAVAL POSTGRADUATE SCHOOL  
September, 1983

Author:

*David A. Waltz*

Approved by:

*David B. Miller*

Thesis Advisor

*David B. Miller*

Second Reader

*Christopher J. R. Moore*

Chairman, Department of Oceanography

*James Dyer*

Dean of Science and Engineering

# ABSTRACT

Pointing error standard deviations for two theodolites, the Wild T-2 and Odom Aztrac, were determined under conditions closely approximating those of range-azimuth or azimuth-azimuth hydrographic surveys. Pointing errors found for both instruments were about 1.3 meters, and were independent of distance. No statistical difference between the errors of the two instruments was found. The accuracy of the interpolation methods used by the National Ocean Service (NOS) for range-azimuth positioning were investigated, and an average inverse distance of about 2.5 meters was observed between interpolated positions and corresponding observed positions. The overall range-azimuth position errors of the two theodolites were then compared to positioning standards of NOS and the International Hydrographic Organization, using assumed ranging standard deviations of 1.0 and 3.0 meters. Both instruments met all standards except the NOS range-azimuth standard for 1:5,000 scale surveys. Interpolated positions may fail to meet more of the standards because of additional inherent error.

## TABLE OF CONTENTS

I.	INTRODUCTION . . . . .	9
	A. THE RANGE-AZIMUTH POSITIONING METHOD . . . . .	9
	B. HYDROGRAPHIC POSITION ERROR STANDARDS . . . . .	12
	C. OBJECTIVES . . . . .	14
II.	ERROR INDICES AND RANGE-AZIMUTH GEOMETRY . . . . .	20
	A. DEFINITIONS . . . . .	20
	1. Blunders . . . . .	22
	2. Systematic Errors . . . . .	23
	3. Random Errors . . . . .	24
	B. TWO-DIMENSIONAL ERROR FIGURES . . . . .	26
	1. Concentric and Eccentric Geometry . . . . .	27
	2. The Error Ellipse . . . . .	29
	3. Root Mean Square Distance . . . . .	33
	4. Circular Standard Error . . . . .	35
	C. THE ERROR OF AN INTERPOLATED FIX . . . . .	37
	1. Interpolation Algorithms . . . . .	37
	2. Error Propagation . . . . .	39
III.	EXPERIMENT DESIGN AND IMPLEMENTATION . . . . .	43
	A. FIELD WORK . . . . .	43
	B. THEODOLITE POINTING ERROR . . . . .	47
	C. INTERPOLATION ALGORITHM EVALUATION . . . . .	49
	D. CHOICE OF EXPERIMENTAL CONDITIONS . . . . .	51
IV.	RESULTS AND DATA ANALYSIS . . . . .	56
	A. DATA PROCESSING SYSTEM . . . . .	56
	B. POINTING ERROR DETERMINATION . . . . .	56
	C. INTERPOLATION EVALUATION . . . . .	64
	D. ANALYSIS OF FACTORS AFFECTING THE RESULTS . . . . .	66



E.	APPLICATION TO POSITION ERROR STANDARDS . . .	72
V.	CONCLUSIONS AND RECOMMENDATIONS . . . . .	79
APPENDIX A:	MEANS AND STANDARD DEVIATIONS OF ACQUIRED DATA SETS . . . . .	85
APPENDIX B:	GEODETTIC POSITION OF HORIZONTAL CONTROL STATIONS . . . . .	91
APPENDIX C:	EMPIRICAL PROBABILITY DENSITY FUNCTION PLOTS . . . . .	92
BIBLIOGRAPHY	. . . . .	98
INITIAL DISTRIBUTION LIST	. . . . .	101

# LIST OF TABLES

I.	Circular Error Formulae . . . . .	36
II.	Data Acquisition Sequence of Events . . . . .	46
III.	Pointing Error Standard Deviation (pooled estimates) . . . . .	58
IV.	Summary of ANOVA Results at 95% Confidence . . . . .	63
V.	Results of Interpolation Evaluation . . . . .	65
VI.	Corrected Aztrac Standard Deviation . . . . .	70
VII.	Experiment Precision and Theodolite Error . . . . .	72
VIII.	Position Standards Comparison . . . . .	78
IX.	3000 Meter Arc . . . . .	85
X.	1500 Meter Arc . . . . .	86
XI.	1000 Meter Arc . . . . .	87
XII.	700 Meter Arc . . . . .	88
XIII.	500 Meter Arc . . . . .	89
XIV.	300 Meter Arc . . . . .	90

## LIST OF FIGURES

1.1	Illustration of Range- Azimuth Positioning . . .	10
1.2	Illustration of Aztrac Shore Station . . .	17
1.3	The Aztrac Transmitting Unit . . .	19
2.1	The Normal Probability Curve . . .	25
2.2	Eccentric Range-Azimuth Geometry . . .	27
2.3	Concentric Range-Azimuth Geometry . . .	28
2.4	Eccentric Error Compensation . . .	29
2.5	Error Ellipse and $d_{rms}$ . . .	31
2.6	A Range-Azimuth Position . . .	32
2.7	Variation of $d_{rms}$ Probability . . .	34
2.8	Example of Angular Interpolation . . .	38
3.1	Sketch of the Survey Area . . .	44
3.2	Lines of Position Observed to the Vessel . . .	45
3.3	Uncertainty of an Observed Error . . .	48
3.4	Interpolation of Angle Only . . .	50
3.5	Interpolation of Angle and Distance . . .	50
4.1	One-Dimensional Difference Between Means . . .	66
4.2	Two-Dimensional Difference Between Means . . .	67
4.3	Probability Density vs. Error . . .	68
4.4	Results Compared to $d_{rms}$ . . .	74
4.5	Results Compared to 90% Probability . . .	76
C.1	Probability Density Plot: 300 m arc . . .	92
C.2	Probability Density Plot: 500 m arc . . .	93
C.3	Probability Density Plot: 700 m arc . . .	94
C.4	Probability Density Plot: 1000 m arc . . .	95
C.5	Probability Density Plot: 1500 m arc . . .	96
C.6	Probability Density Plot: 3000 m arc . . .	97

## I. INTRODUCTION

### A. THE RANGE-AZIMUTH POSITIONING METHOD

The fundamental purpose of a hydrographic survey is defined by Ingham (1974) as being to "depict the relief of the seabed, including all features, natural and manmade, and to indicate the nature of the seabed in a manner similar to the topographic map of land areas." He goes on to describe two factors defining a single point on the seabed:

(i) "The position of the point in the horizontal plane in, for example, latitude and longitude, grid co-ordinates or angles and distances from known control points.

(ii) The depth of the point below the sea surface, corrected for the vertical distance between the point of measurement and water level and for the height of the tide above the datum or reference level to which depths are to be related."

Thus the hydrographer must answer the two primary questions of "how deep" and "where" for each of the thousands of soundings acquired on every survey. Because every area to be surveyed has different geophysical characteristics and levels of use, the hydrographer must possess a suite of tools and techniques to accomplish each survey. A survey of a large metropolitan harbor requires different equipment and measurement precision than one for a deep ocean area.

Only the first of Ingham's two factors cited above is considered, and it is further narrowed in scope to techniques used in the most precise surveys. Such a survey might be one of a winding, narrow river carrying deep draft vessels, or perhaps a very large scale survey of an inner harbor. Both areas require the highest positioning accuracy and a minimum of shore control stations.

Any method of positioning employs the intersection of lines of position (LOP's) to construct a fix. Although advanced methods may use multiple LOP's, traditional hydrography uses the simple intersection of two lines to fix the vessel's position. The vessel is located somewhere along each of two lines of position, and the only point satisfying these conditions is the intersection of the lines.

The error associated with one of the simplest positioning methods, that of the two LOP range-azimuth fix, which is illustrated in Figure 1.1, is analyzed.

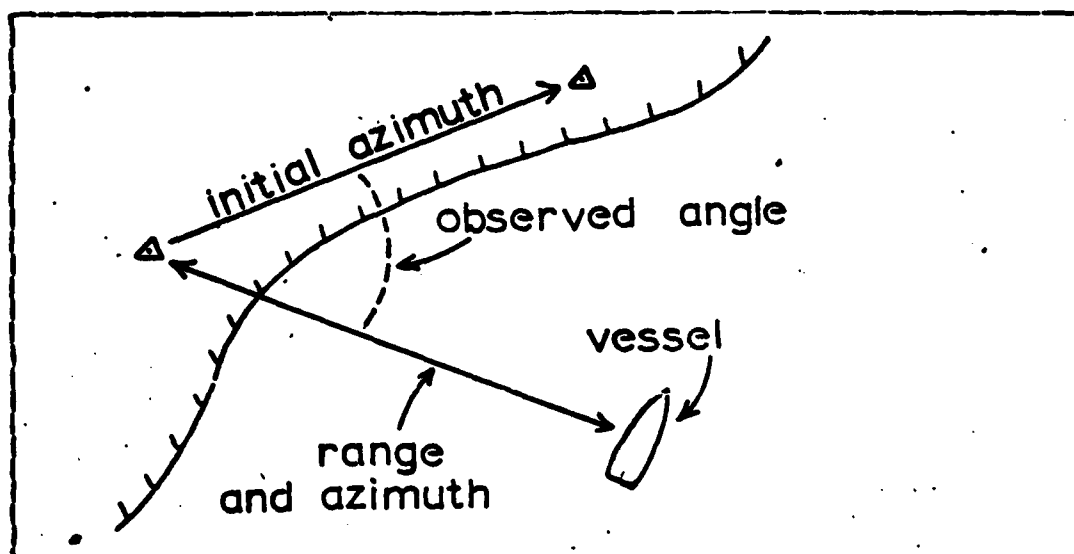


Figure 1.1 Illustration of Range- Azimuth Positioning.

Also called the rho/theta method, range-azimuth positioning consists of the observation of a distance and an azimuth to a vessel from either one or two known locations [Umbach, 1976]. An example of this method is the use of radar aboard ship. A relative position for a radar contact is determined by observing a radar range and azimuth, or a radar range and visual azimuth, to a contact. The two lines of position

always intersect at right angles because the observation is made from a single point, and this concentric geometry provides the strongest fix possible. Mariners also know that the fix obtained via a visual azimuth is stronger than the one using a radar azimuth, because the visual bearing is more accurate.

This example shows the advantages that make the range-azimuth method popular for hydrography. It provides the geometrically strongest possible fix, and only one location on shore need be occupied to control the survey. Such a positioning method is ideal in harbors or rivers where maximum accuracy is needed but where obstructions make other types of fix geometry impractical. In 1982 the U.S. National Ocean Service (NOS) obtained twenty thousand linear nautical miles of launch hydrography, and sixty percent of this was controlled by the range-azimuth method [Wallace, 1983].

There are limitations associated with this method just as with any fix geometry. It is labor intensive and requires more radio communication (to establish fix timing) than most other methods. In totally nonautomated situations, distances to the survey vessel are recorded manually aboard the vessel, and azimuths are recorded ashore by the theodolite observer at prescribed intervals. These fix data are later put into computer compatible digital form via a process called logging. Manual recording of these fix data are generally too slow to position every sounding. Therefore, individual sounding positions must be interpolated from the observed fixes.

Systems have been designed that have an intermediate level of automation. The NOS Hydroplot System is an example of this type [Wallace, 1967]. When used in the range-azimuth mode, the vessel is usually steered along arcs of constant range from the theodolite station, and the

Hydroplot System automatically records a distance measurement for each sounding. Azimuths are not telemetered to the vessel but are relayed over voice radio and are manually entered into the computer system. Since the maximum data rate is about two angles per minute, the interpolation of angles for sounding positions between fixes is necessary.

Recently a digital theodolite, the Odom Aztrac, has been developed which can record and telemeter angles with great speed -- up to ten angles per second [Odom Offshore Surveys, Inc., 1982]. A computer system aboard the survey vessel can thus record and plot an observed position for each sounding. This rapid position fixing, combined with a computer's ability to provide cross-track error indications to the helmsman, enables the hydrographer to systematically cover a survey area with maximum efficiency by running straight and parallel sounding lines.

The Aztrac system is still considered a semiautomated system because an observer is required to manually track the vessel with the theodolite. Two fully automated range-azimuth systems which feature fully automatic tracking have been developed. One is the Polarfix system developed by Krupp-Atlas Elektronik in Germany [Smith, 1983], and the other is the Artemis system developed by Christiaan Huygenslaboratorium in the Netherlands [Newell, 1981].

## **B. HYDROGRAPHIC POSITION ERROR STANDARDS**

Historically, most national hydrographic organizations, as well as the International Hydrographic Organization (IHO), have used linear plotting error at the scale of the survey to be the standard for sounding position accuracy. Prior to 1982, the standards recommended by IHO [IHO, 1968] were:

"The indicated repeatability of a fix  
(accuracy of location referred to shore

control) in the operating area, whether observed by visual or electronic methods, combined with plotting error, shall seldom exceed 1.5 mm (0.05 in) at the scale of the survey."

The IHO recently published new recommendations for error standards [IHO, 1982] which are:

"... any probable error, measured relative to shore control, shall seldom exceed twice the minimum plottable error at the scale of the survey (normally 1.0 mm on paper)."

Neither of the IHO standards make any reference as to what probability level they apply. Munson (1977) interpreted the words "shall seldom exceed" in the above statements to mean "less than 10% of the time", which seems reasonable. The 1982 IHO standard is somewhat confusing due to its use of both the terms "seldom exceed" and "probable error". The latter term is associated with a 50% probability by most statisticians including Greenwalt (1971). However, the author of these standards, Commodore A. H. Cooper, RAN (ret'd), has stated that he intended no statistical significance to the term "probable error" [Wallace, 1983].

The NOS has not yet incorporated the latest IHO standards, but such action is being considered in some form [Wallace, 1983]. Current NOS standards have been developed to ensure that "accuracies attained for all hydrographic surveys conducted by NOS shall equal or exceed the specifications" of the 1968 IHO standards [Umbach, 1976]. Unlike the international standards, the NOS standards for all electronic positioning systems use the concept of root mean square error ( $d_{rms}$  or  $rms_e$ ), which has a somewhat variable probability of between 68.3 and 63.2 percent. The NOS standards for fully visual and for hybrid (combination electronic and visual) positioning have no explicit reference to probability.



Specific operational standards for range-azimuth positioning have been neglected by many hydrographic organizations. However, NOS [Umbach, 1976] requires the following observational procedures be followed for all range-azimuth positions.

"Objects sighted on should be at least 500 m from the theodolite... the azimuth check should not exceed one minute of arc... observed azimuths or directions to the sounding vessel for a position fix shall be read to the nearest 1 min of arc or better if necessary to produce a positional accuracy of 0.5 m at the scale of the survey."

Since the range-azimuth method is classified as a hybrid positioning system, it is not referenced to any particular probability, but a reasonable assumption may be made that the  $d_{rms}$  concept also applies in this case.

The U.S. Naval Oceanographic Office (NAVOCEANO) also requires that its surveys meet the standards of the NOS Hydrographic Manual. The Army Corps of Engineers presently have no formal positioning requirements that must be met by all districts, although draft specifications are being written at this time [Hart, 1983]. The range-azimuth technique and its applicability to Corps of Engineers surveys is discussed in Hart (1977). No specific requirements for range-azimuth positioning could be found for either the Canadian Hydrographic Service or the British Hydrographic Service. Palikaris (1983) also reports no published standards for these organizations.

### C. OBJECTIVES

All position error standards using an explicit probability are based on the idea that an observation is a normally distributed random variable with zero mean and standard deviation  $\sigma$ . These standards require a value for

the standard deviation of the component lines of position that make up the fix. The standard deviation is a value such that there is a 68.27% probability of an observation falling within  $\pm 1\sigma$  of the mean. It is unfortunate that often the  $1\sigma$  values of a hydrographic measurement are simply not known, or known only for ideal conditions and provided by manufacturers who have a vested interest in the measuring instrument.

This paper and experiment, then, has as its primary purpose the determination of a pointing error standard deviation for two theodolites used to measure azimuths under hydrographic conditions. One instrument (the Wild T-2) is the standard used by NOS field units. The other (the Odom Aztrac) is a new digital telemetering theodolite, which may prove useful in automating the presently tedious manual methods. No estimation of standard deviation has ever been made on these devices under typical range-azimuth conditions.

The T-2 is the standard instrument used by NOS surveying parties for land surveying and, to a lesser extent, hydrography. It is a very precise instrument used in third-order horizontal control and provides an angular resolution of one second of arc. However, it does possess features that are less than ideal for range-azimuth work. The horizontal tangent screw of this instrument is awkward for range-azimuth surveying because it is not an infinite gearing device. The observer often encounters the end of the drive mechanism, stopping the instrument's movement while tracking the vessel. A solution to this problem for many observers is to track the vessel with the tangent screw unclamped, then clamp the screw only seconds before the fix occurs.

The inverted image feature of the T-2's in use by NOS simplifies the optical system and reduces optical error. This is satisfactory for land survey work but creates some

confusion when tracking a fast moving vessel. This is because the observer sees an image of the survey boat upside down and moving apparently in the opposite direction from its actual movement. Another disadvantage is that the mechanism for reading the horizontal circle of a T-2 is more complicated than desired for the rapid observations necessary in hydrographic survey work. The operator is required to stop tracking the vessel, remove his eye from the telescope, and use an auxiliary eyepiece to read the angle. There is a practical limit of about 30 seconds to the speed with which successive angles can be observed and read. The particular unit tested was serial number 30504.

The Odom Aztrac theodolite is a semi-automated, line-of-sight angle measuring system. The Aztrac system consists of a Wild T-16 theodolite (serial number 2534880 was tested) which was modified for infinite tangent drive and to provide angular information in a digital format. The shore unit decodes the observed angle, determines the direction of rotation of the instrument and displays the angle on its front panel. The angle is then converted to binary coded decimal (BCD) format and used to frequency shift key (FSK) an FM transmitter to link the data with the survey vessel. The data is transmitted at the rate of 10 angles per second. On board the vessel the Aztrac receiver converts the received data to parallel form and displays it on the front panel for manual recording. For automated recording or processing by onboard computer a serial data output is provided. The Aztrac has an angular resolution of 0.01 degree (36 arc seconds) [Odom, 1983].

With the notable exception of angular resolution, this theodolite is more appropriate for range-azimuth hydrography than the Wild T-2. It has an erect image and infinite tangent screw which allow the vessel to be constantly tracked. Its digital output requires no action on the



Figure 1.2 Illustration of Aztrac Shore Station.

operator's part to record observed angles. An additional positive feature of the digital output is the ability to rapidly zero the instrument on an initial pointing. This is done by pressing a manual reset button on the instrument control panel. Figures 1.2 and 1.3 show photographs of the Aztrac equipment. Figure 1.2 illustrates a typical shore station. The observer is adjusting the Aztrac instrument, and the transmitter unit is on the ground to the right of the Aztrac tripod. The distance measuring equipment is mounted on a tripod behind the observer, and the Aztrac transmitting antenna is at the top of a pole on the extreme right of the photograph. Figure 1.3 shows the Aztrac transmitter unit, with its digital angular display in hundredths of a degree. Both photographs were provided by Odom Offshore Surveys, Inc.

A second objective of this paper is to evaluate the interpolation methods used by the NDS for range-azimuth work. The availability of the digital theodolite, with its direct measurement of all positions, enabled a comparison of observed and interpolated fixes to be made. This made possible an estimate of whether interpolated positions meet required accuracy standards, and whether direct measurement of all positions is needed. The estimate presented here was not made statistically rigorous so that the thesis could be kept to a manageable size. More theoretical statistical work is needed to fully reduce the interpolation data.

The final objective of this investigation is to compare the position errors of these two instruments with the various position error standards discussed in section B of this chapter. The conclusions resulting from this objective will assist the hydrographer to select equipment and operating conditions that meet required position error standards.

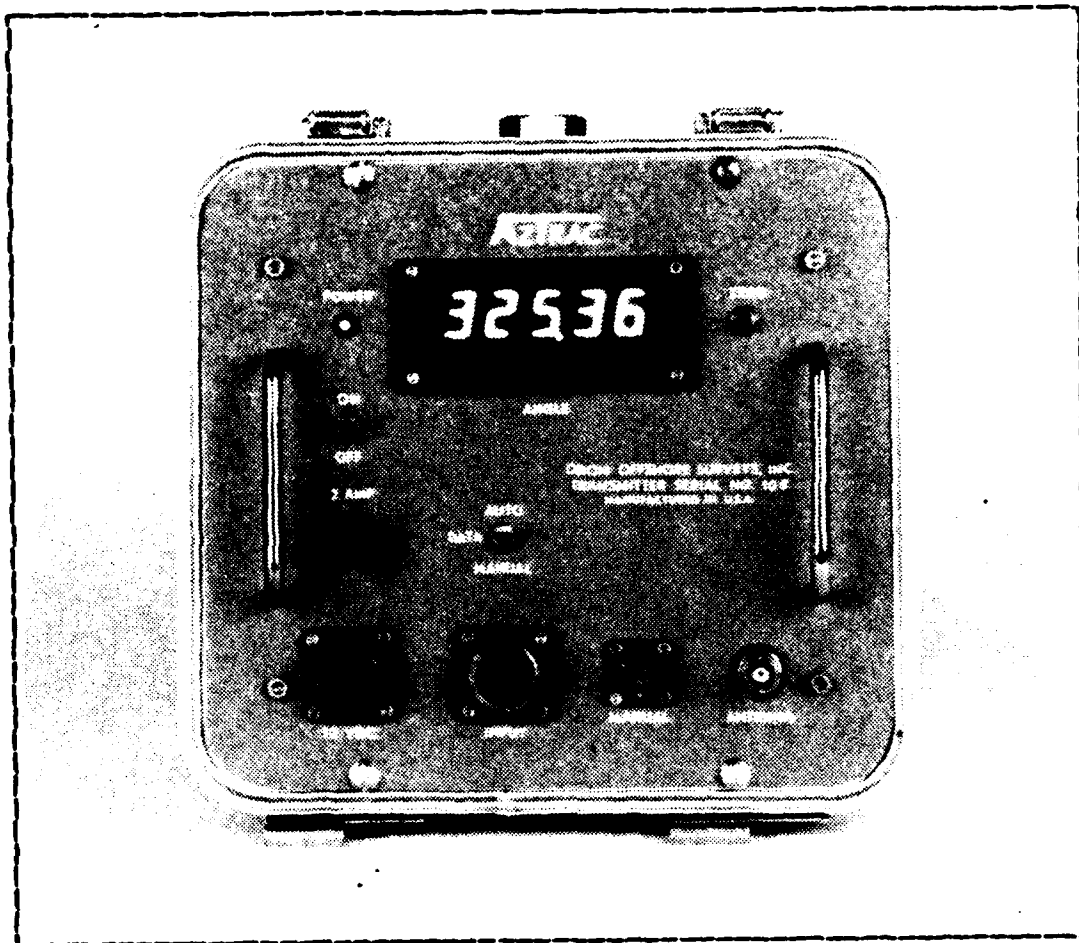


Figure 1.3 The Aztrac Transmitting Unit.

## II. ERROR INDICES AND RANGE-AZIMUTH GEOMETRY

The method of range-azimuth positioning is usually selected for large scale surveys because of its simplicity and accuracy. This is the result of both angle and distance measurement devices being co-located, with the intersection of the two lines of position always being ninety degrees. In practice, however, the co-location of both instruments is often not achieved. The result is an eccentric geometry for the position fix. This section will analyze the geometry of both eccentric and concentric fixes. Position error indices in common use will be reviewed and analyzed for the special cases of range-azimuth methods, and the error of an interpolated fix will be derived.

### A. DEFINITIONS

Although a complete and general treatment of error theory will not be presented, some basic definitions are necessary to understand the data analysis presented here. The ideas in this section are included in many basic statistics textbooks, and were specifically drawn from Wonnacott (1977), Bowditch (1977), Heinzen (1977), Kaplan (1980), and Davis (1981).

Error may be defined as "the difference between a specific value and the correct or standard value" [Bowditch, 1977], or as "the difference between a given measurement and the "true" or "exact" value of the measured quantity" [Davis, 1981]. Mathematically it can be defined as:

$$e = x_i - T \quad (2.1)$$

where  $e$  is the error,  $x_i$  is an observation, and  $T$  is the "correct" or "true" value. The word error implies that there is a known true value for a quantity, with which a measurement may be compared to find the "error" associated with that measurement. Since the true value of a measured quantity is rarely known, the term "error" is not precisely correct. Davis (1981) states that it is more appropriate to speak of the theory of observations rather than the theory of errors, but it can be shown that the difference between the two is largely one of semantics.

A single measurement of a particular quantity may be considered sufficient for many purposes, even if it is known that additional measurements will probably be slightly different than the first. If the quantity to be measured is of sufficient importance, then multiple measurements are made and the sample mean,  $\bar{X}$ , is used. Each of these multiple measurements can be considered a numerical value for a random variable. A random variable is one that takes on a range of possible values, each associated with a particular probability.

The sample mean may be expressed mathematically by equation 2.2 [McNacott, 1977]:

$$\bar{X} = \frac{1}{n} \sum_{i=1}^n x_i \quad (2.2)$$

where  $n$  is the sample size. If the sample size were increased without limit ( $n \rightarrow \infty$ ), equation 2.2 would give the population mean  $\mu$ . The sample mean is always an estimate of the population mean, which is never directly computed. This leads to the concept of the residual,  $v$ , which is the difference between the estimate  $\bar{X}$  of the population mean and the observation  $x_i$ . This is shown in equation 2.3.



$$v = \bar{X} - x_i \quad (2.3)$$

The residual is computationally the negative of the error. Nevertheless, equation 2.3 is more appropriate because it uses an estimate,  $\bar{X}$ , of the unknowable population mean  $\mu$ . The presence of  $\bar{X}$  in equations 2.3 implies that multiple measurements have been made, and allows a particular confidence to be assigned to the estimate of  $\mu$  depending on the number of such measurements. Because the word error is still used in much of the hydrographic profession, it will be used interchangeably in this paper with the term residual. It is important, however, to understand that the concept of the residual, whatever its name may be, is fundamental to any measurement operation.

Errors are classically divided into three groups: blunders, systematic error, and random errors [Greenwalt, 1962]. Bowditch (1977) and Davis (1981) do not classify errors as including blunders, but like the term error itself, the distinction is largely a semantic one. Ideally blunders and systematic errors are completely eliminated from the data. The most precise measurements reduce random error as much as possible, but it can never be completely eliminated.

### 1. Blunders

Blunders are mistakes that are "usually gross in magnitude compared to the other two types of errors" [Davis, 1981], and are most often caused by carelessness on the part of the observer, or by grossly malfunctioning observing equipment. They are usually detected and eliminated by procedural checks during the data acquisition process. The recognition of a blunder is not always easy, since a blunder "may have any magnitude, and may be positive or negative" [Bowditch, 1977].

## 2. Systematic Errors

Systematic errors are defined by Davis (1981) as those that occur "according to a system which, if known, can always be expressed by mathematical formulation." This mathematical model results in correctors that are applied to all measurements obtained, thus eliminating the systematic errors from the observations. The model may be as simple as a constant corrector subtracted from lengths obtained with a steel tape, or it may be as complicated as modelling the effects of atmospheric refraction on electronic distance measuring equipment.

If the systematic error is such that it cannot be modelled, it is then estimated by a process known as calibration. Kaplan (1980) defines calibration as the process of comparing the measuring instrument against a "known" standard. The word "known" is usually operationally defined as a measurement operation or instrument that is much more accurate than the one being calibrated. The difference between the observed and standard value is used as an estimate of the total effect of all systematic errors present. This process is very close to the classical concept of "errors" presented above, and is entirely proper for use in the correction of systematic errors [Davis, 1981]. Of course, one must be careful to apply the corrector only to those measurements made under the same conditions as the calibration.

A systematic error found in theodolite or sextant observations is known as the personal error of the observer [Mueller, 1969], [Bowditch, 1977]. This type of error is rarely quantified for hydrographic applications, but nevertheless it does exist. The observer must rely on the senses of hearing and vision to make measurements, which vary between individuals as well as with time in one individual.

Some personal errors are constant and some are erratic [Davis, 1981]. These errors are minimized by training and standardizing observational procedures. The best way to eliminate personal error is by the use of completely automated observation equipment.

### 3. Random Errors

"Random errors are chance errors, unpredictable in magnitude or sign", and are "governed by the laws of probability" [Bowditch, 1977]. If one assumes that all blunders and systematic errors have been removed from the observations, the remaining values can be regarded as sample values for a random variable. As noted earlier, a random variable can take on a range of values, each associated with a particular probability. A random error has high probability of being close to the population mean,  $\mu$ , and a low probability of being very much different than  $\mu$  [Greenwalt, 1962].

A probability density function expresses the relation between a value for a random variable and the probability of its occurrence. Hydrographic survey measurements often use the normal or Gaussian probability density function. A concise explanation of this function is given in Greenwalt (1962) and Kaplan (1980). The function itself is given as equation 2.4, where  $p(v)$  is the probability of the occurrence of a particular residual  $v$ , and  $\sigma^2$  is the population variance which is approximated by the sample variance,  $S^2$ , given by equation 2.5.

$$p(v) = \frac{1}{\sigma\sqrt{2\pi}} \exp\left[-\frac{v^2}{2\sigma^2}\right] \quad (2.4)$$

$$S^2 = \frac{1}{n-1} \sum_{i=1}^n (\bar{x} - x_i)^2 \quad (2.5)$$

To find the probability of a residual falling between two residuals  $v_1$  and  $v_2$ , equation 2.4 must be integrated over the interval  $v_1$  to  $v_2$ . This corresponds to the area under the gaussian curve between those two points, as is shown in Figure 2.1. If  $p(v)$  were integrated from  $-1\sigma$  to  $+1\sigma$ , the area under the curve would be 68.27% of the total area. This means that there is a 68.27% probability of a particular residual falling between plus or minus one standard deviation of the mean, where the standard deviation,  $\sigma$ , is defined as the square root of the variance given in equation 2.5.

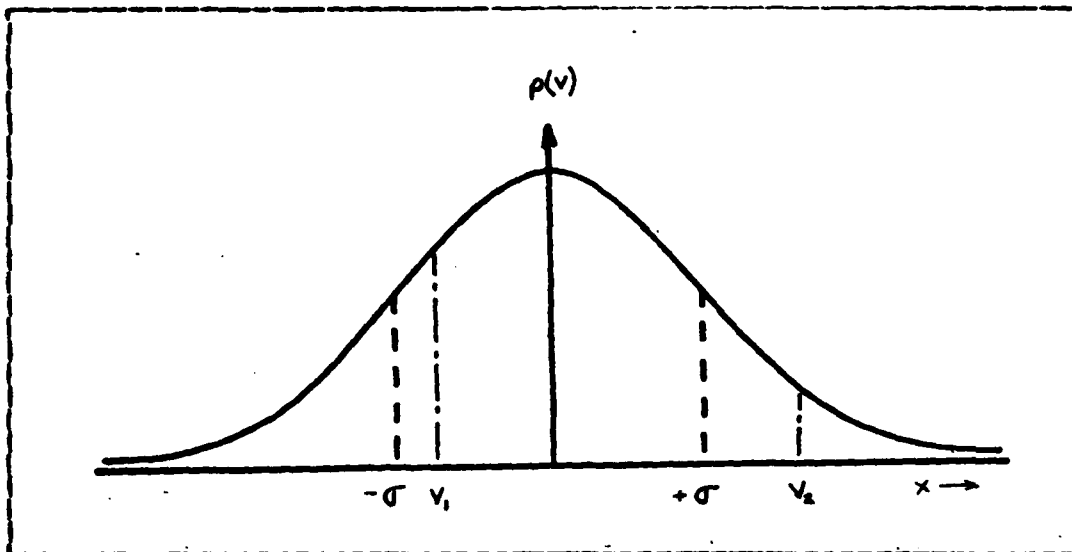


Figure 2.1 The Normal Probability Curve.

The combined effect of blunders, systematic errors and random errors can now be seen in overview. If it is assumed that blunders and systematic errors have been completely eliminated from a set of observations, there remain only random errors. If the sample size is large enough, then the sample mean and variance are good

approximations of the population mean and variance. That is, there is a 68.27% probability that any future measurements made under the same conditions will not fall farther than plus or minus one standard deviation from the mean.

## B. TWO-DIMENSIONAL ERROR FIGURES

The two-dimensional error of a position, as applied to the special case of range-azimuth fixes, must next be examined. Two figures, the ellipse and the circle, are used to characterize two-dimensional error. The "error diamond" is also sometimes used but has no statistical significance [Thomson, 1977]. The error ellipse is discussed first since it is the most general index of error. Another is root mean square distance ( $d_{rms}$ ), also known as root mean square error [Bowditch, 1977], which is the radius of a circular figure commonly used in hydrography. It is the error index used for NOS positioning standards [Umbach, 1976]. A second circular figure, known as circular standard error, is also examined briefly because of the ease of converting it to circular figures which have different probabilities.

For clarification of the issues involved in this section, the following assumptions are made.

- (i) Only random errors are considered.
- (ii) Errors associated with each LOP are normally distributed.
- (iii) Errors are independent.
- (iv) Errors are limited to the two-dimensional case.
- (v) LOP's are straight lines at their point of intersection.

These are the same assumptions made by Kaplan (1980), except that Kaplan allows systematic error to be considered in assumption (i). This appears to be an oversight since the remainder of his discussion, from which this section draws heavily, considers only random error.

#### 1. Concentric and Eccentric Geometry

Before proceeding further into a discussion of error figures, it is necessary to examine the two special cases of range-azimuth positioning, that of eccentric and concentric geometry. Each is illustrated in Figures 2.2 and 2.3.

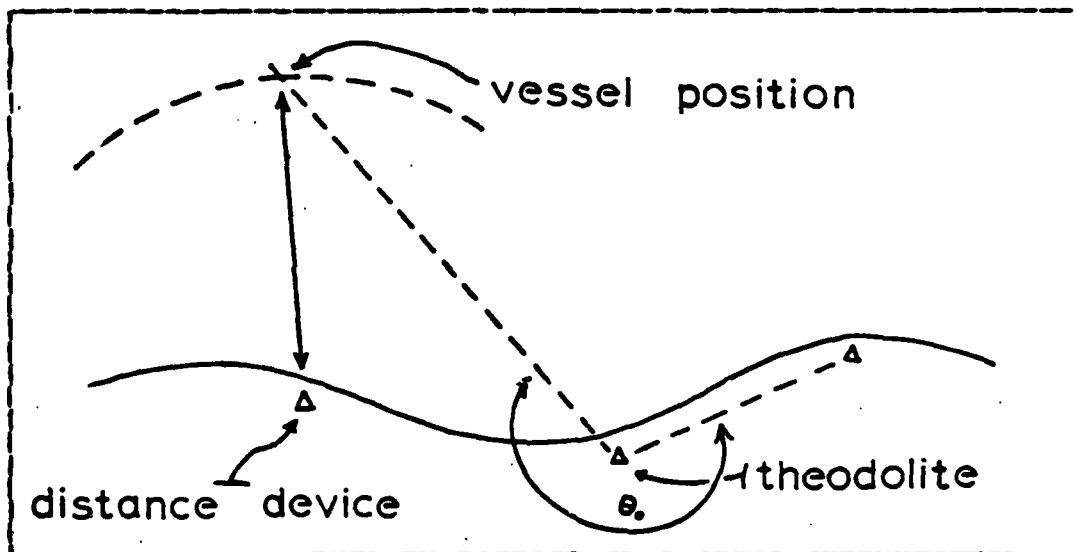


Figure 2.2 Eccentric Range-Azimuth Geometry.

In actual practice the geometry used is often eccentric, but the concentric assumption is made. This is because it is usually difficult to co-locate both theodolite and ranging equipment. Hence, they are offset one or two meters from each other. It should be noted that this assumption will introduce a systematic error in all

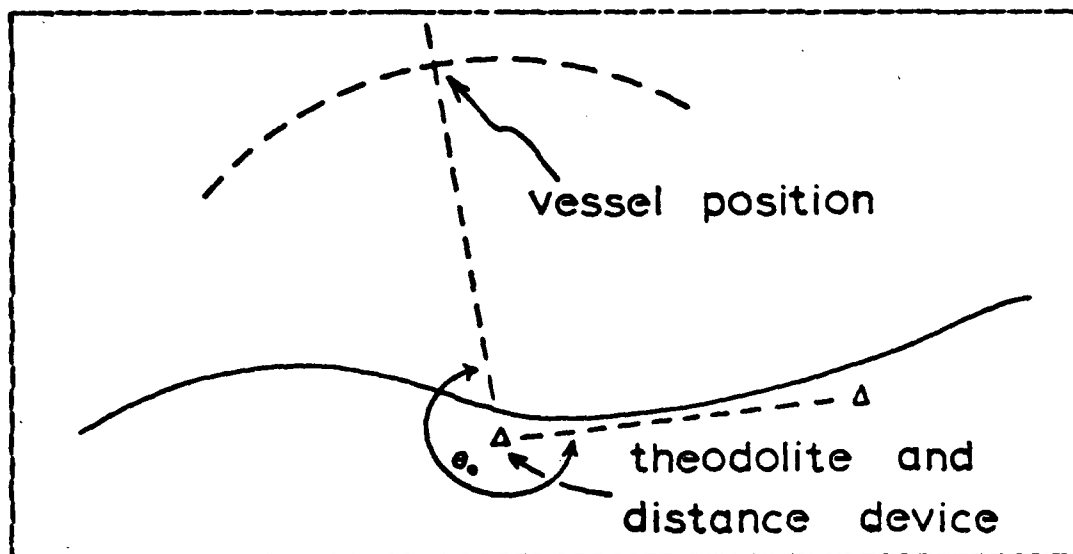


Figure 2.3 Concentric Range-Azimuth Geometry.

positions, which must be eliminated before an analysis of random errors can be made. The systematic error is often ignored (by use of the concentric assumption) if the total uncompensated error is within the tolerance of the standards being used. An algorithm for eliminating this error is shown in Figure 2.4 and given by equation 2.6. This algorithm assumes that the size of  $d$  in Figure 2.4 is small compared to  $r$ .

$$c = d \cos \phi \quad (2.6)$$

where:

$c$  = the corrector to be applied to  $r$

$r$  = observed range to the vessel

$d$  = distance between theodolite and ranging device

$\phi$  = the angle between the visual LOP and the line connecting the two stations

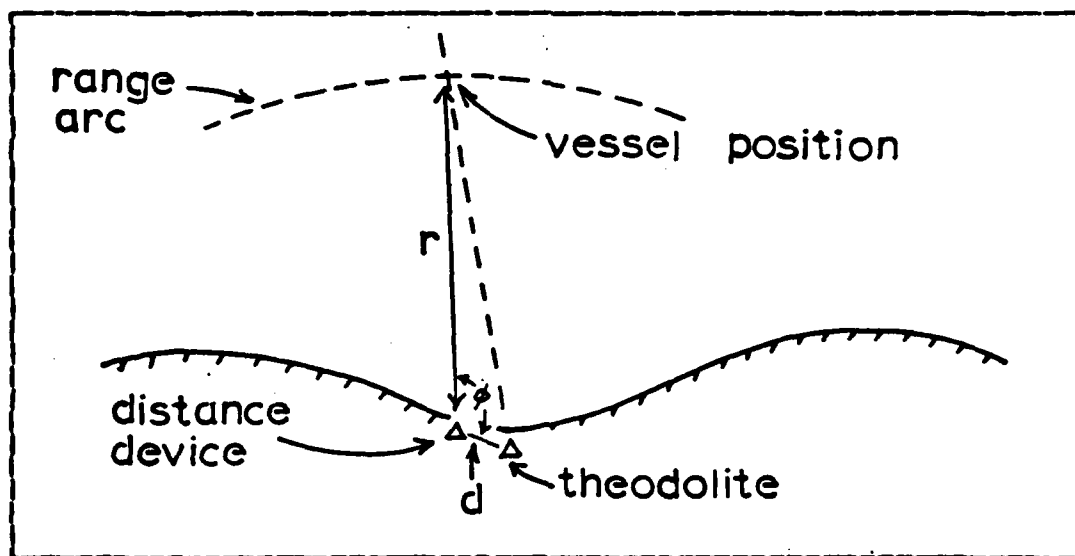


Figure 2.4 Eccentric Error Compensation.

## 2. The Error Ellipse

Detailed discussions of the development of the error ellipse can be found in many references, especially in Greenwalt (1962) and in Burt (1966). This paper will only present enough background to apply the error ellipse concept to two LOP range-azimuth positioning. The error ellipse formed when multiple LOP observations are made is not considered here.

A range-azimuth position is formed by the intersection of two LOP's, each having an associated standard deviation. By applying the two-dimensional normal distribution to the errors, elliptical contours of equal probability density are formed. The contours center on the intersection point of the lines of position. This is illustrated in Figure 2.5, and shown mathematically by

$$p(v_a, v_b) = \frac{1}{2\pi\sigma_a\sigma_b} \exp \left[ -\frac{1}{2} \left( \frac{v_a^2}{\sigma_a^2} + \frac{v_b^2}{\sigma_b^2} \right) \right] \quad (2.7)$$



where:

- $v_a$  = residual (error) in the direction of  $\sigma_a$
- $v_b$  = residual (error) in the direction of  $\sigma_b$
- $\sigma_a$  = length of the semi-major axis
- $\sigma_b$  = length of the semi-minor axis

It can be shown that

$$\left( \frac{v_a^2}{\sigma_a^2} + \frac{v_b^2}{\sigma_b^2} \right) = K^2 \quad (2.8)$$

where

$$K^2 = -2 \ln \left[ p(v_a, v_b) \sigma_a \sigma_b 2\pi \right] \quad (2.9)$$

"For values of  $p(v, v)$  from 0 to  $\infty$ , a family of equal probability density ellipses are formed with axes  $K \sigma_a$  and  $K \sigma_b$ " [Greenwalt, 1962]. The probability density function in equation 2.7, when integrated over a particular area, becomes the probability distribution function. This yields the probability that the residuals  $v_a$  and  $v_b$  will occur simultaneously within that region. This probability distribution function of an ellipse is given by

$$P(v_a, v_b) = 1 - e^{-K^2/2} \quad (2.10)$$

The solution of equation 2.8 for different values of  $K$  yields different probabilities. For example, for 39.35% probability, the axes of the ellipse are  $1.000 \sigma_a$  and  $1.000 \sigma_b$  [Greenwalt, 1962]. In other words, a one-sigma error ellipse around a measured position indicates a 39.35% probability that the position is actually within that ellipse.

It is seen in Figure 2.5 that the standard deviations  $\sigma_1$  and  $\sigma_2$  of the measured LOP's are not the same as the standard deviations  $\sigma_a$  and  $\sigma_b$  of the error ellipse. A

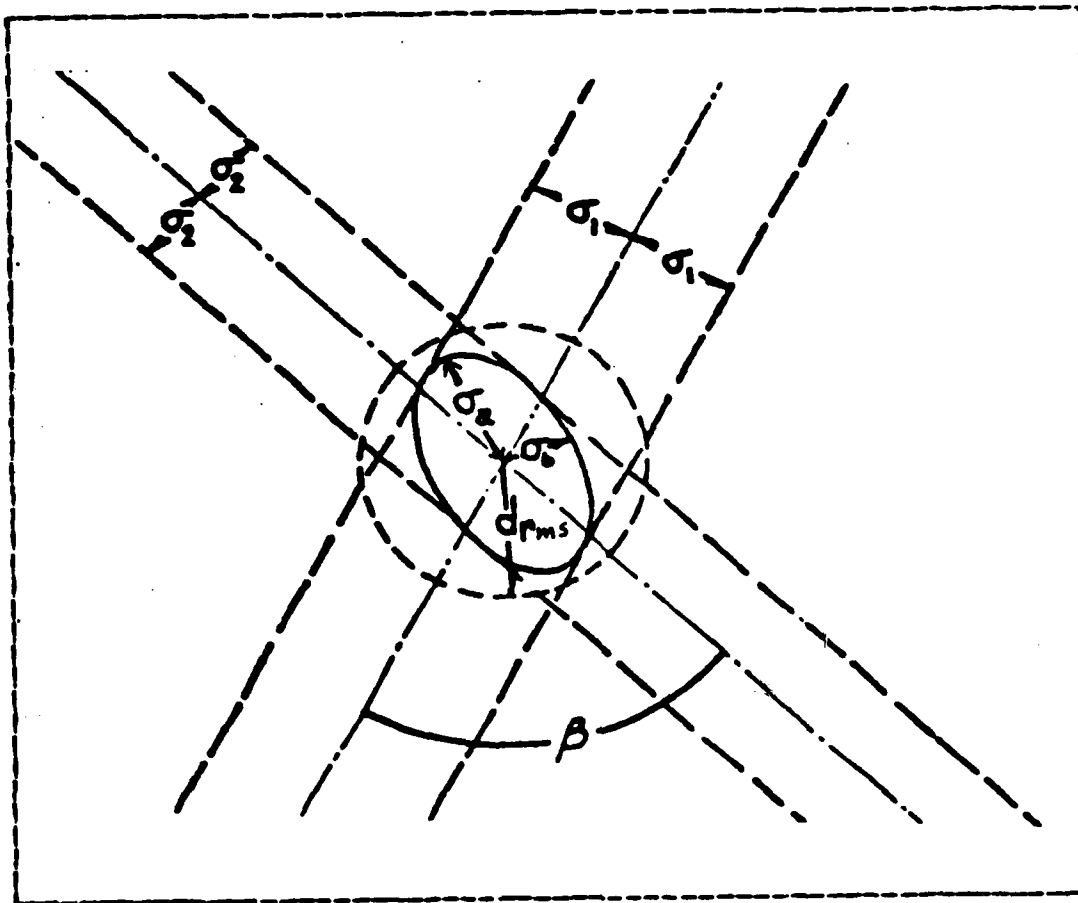


Figure 2.5 Error Ellipse and  $d_{rms}$ .

coordinate transformation is required to obtain them. This transformation is found in Heinzen (1977) and will not be discussed here. Results of the transformation are presented in equations 2.11 and 2.12, from Bowditch (1977).

$$\sigma_a^2 = \frac{1}{2 \sin^2 \beta} \left[ \sigma_1^2 + \sigma_2^2 + \sqrt{(\sigma_1^2 + \sigma_2^2) - 4 \sin^2 \beta \sigma_1^2 \sigma_2^2} \right] \quad (2.11)$$

$$\sigma_b^2 = \frac{1}{2 \sin^2 \beta} \left[ \sigma_1^2 + \sigma_2^2 - \sqrt{(\sigma_1^2 + \sigma_2^2) - 4 \sin^2 \beta \sigma_1^2 \sigma_2^2} \right] \quad (2.12)$$

where:

$\sigma_a$  = length of the semi-major axis

$\sigma_b$  = length of the semi-minor axis

$\sigma_1$  = standard deviation of the range LOP

$\sigma_2$  = standard deviation of the angle LOP

when converted to distance units

$\beta$  = angle of intersection of LOP's

For range-azimuth positioning,  $\sigma_1$  and  $\sigma_2$  are not equal.  $\sigma_1$  is the error in distance measurement, and it is dependent on the equipment used for ranging. A diagram of a range-azimuth position is shown in Figure 2.6.

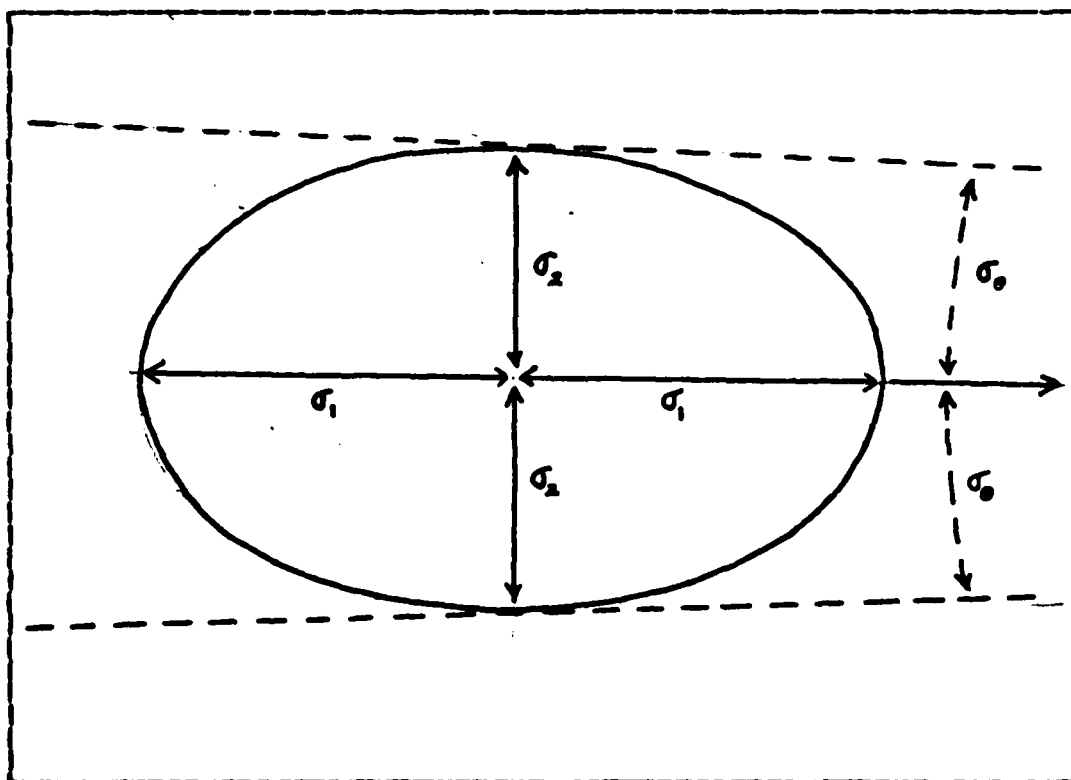


Figure 2.6 A Range-Azimuth Position.

The error in the visual LOP,  $\sigma_2$ , is a function of the angular error of the theodolite and the distance to the vessel, where  $r$  is the distance and  $\sigma_\theta$  is the angular standard deviation of the theodolite, in units of degrees. This is given by equation 2.13, which is a modification from Heinzen [1977]. Heinzen uses the term angular resolution in place of the more correct  $\sigma_\theta$ .

$$\sigma_2 = \frac{r \sigma_\theta}{57.296} \quad (2.13)$$

The error ellipse concept can now be applied to the eccentric geometry by using equation 2.11, 2.12, and 2.13 directly. In the concentric case, since the angle of intersection,  $\beta$ , is always ninety degrees, equations 2.11 and 2.12 can be simplified to equations 2.14 and 2.15.

$$\sigma_a^2 = \frac{1}{2} \left[ \sigma_1^2 + \sigma_2^2 + \sqrt{(\sigma_1^2 + \sigma_2^2) - 4 \sigma_1^2 \sigma_2^2} \right] \quad (2.14)$$

$$\sigma_b^2 = \frac{1}{2} \left[ \sigma_1^2 + \sigma_2^2 - \sqrt{(\sigma_1^2 + \sigma_2^2) - 4 \sigma_1^2 \sigma_2^2} \right] \quad (2.15)$$

### 3. Root Mean Square Distance

Root mean square distance ( $d_{rms}$ ) is presented here because of its common use in hydrography. It is not commonly known among hydrographers that unlike the error ellipse,  $d_{rms}$  has a variable probability depending on the eccentricity of its associated error ellipse, and ranges from 68.3% to 63.2%, as shown in Figure 2.7 from [Burt, 1977]. Eccentricity is defined as the ratio of the semi-minor to the semi-major axes of the error ellipse. Root mean square distance is also called Mean Square Positional Error (MPSE) by Greenwalt (1962), who recommends

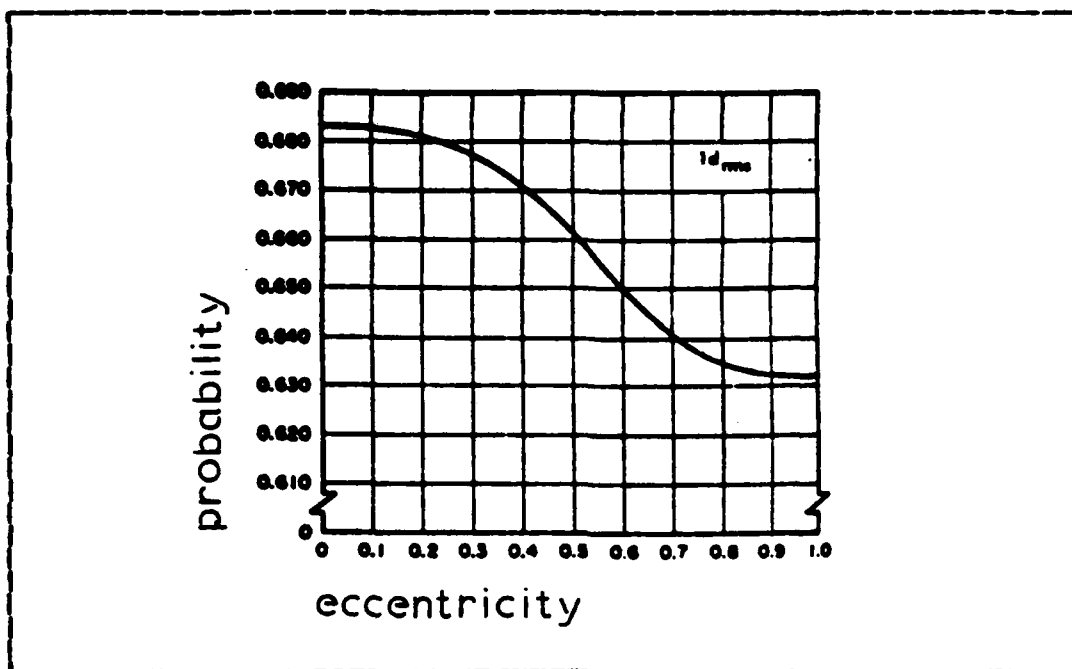


Figure 2.7 Variation of  $d_{rms}$  Probability.

that this index not be used because of its variation in probability.

Root mean square distance is defined in Bowditch (1977) as equation 2.16. An alternative form is given by Heinzen (1977) as equation 2.17. If the errors are assumed independent, the correlation coefficient  $\rho_{12}$ , is zero and equation 2.17 is reduced to equation 2.18. An alternate method of arriving at equation 2.18 is to substitute equations 2.11 and 2.12 directly into equation 2.16.

$$d_{rms} = \sqrt{\sigma_a^2 + \sigma_b^2} \quad (2.16)$$

$$d_{rms} = \frac{1}{\sin \beta} \sqrt{\sigma_1^2 + \sigma_2^2 + 2\rho_{12} \sigma_1 \sigma_2 \cos \beta} \quad (2.17)$$

$$d_{rms} = \frac{1}{\sin \beta} \sqrt{\sigma_1^2 + \sigma_2^2} \quad (2.18)$$

If concentric geometry is assumed, the angle  $\beta$  is equal to ninety degrees and equation 2.18 is reduced to equation 2.19.

$$d_{rms} = \sqrt{\sigma_1^2 + \sigma_2^2} \quad (2.19)$$

Substituting equation 2.13 into equation 2.19, the final form for range-azimuth  $d_{rms}$  is obtained.

$$d_{rms} = \sqrt{\sigma_1^2 + \frac{r \sigma_0}{57.296}} \quad (2.20)$$

#### 4. Circular Standard Error

Circular standard error has experienced little use in hydrography but is valuable because it allows easy conversion between circles of different probability. It is derived in Greenwalt (1962) and given by equation 2.21. It should be noted that this equation is only an approximation, although a very good one.

$$\sigma_c = 0.5000 (\sigma_a + \sigma_b) \quad (2.21)$$

Circular standard error has a probability of 39.35% for a completely circular error ellipse. It is preferred over  $d_{rms}$  because it can be converted to other circular error indices of different probability by a constant conversion factor, as long as the ratio of  $\sigma_b/\sigma_a$  is between 0.2 and 1.0. The equation for circular standard error, and for other circular error figures, is given in Table I, which is taken directly from Greenwalt (1962). This table gives all error indices in terms of either  $\sigma_c$  or the error ellipse

**TABLE I**  
**Circular Error Formulae**

Precision Index	Percentage Probability	Formula
Circular Standard Error	39.35%	$\sigma_c = 0.5000 (\sigma_x + \sigma_y)$ when $\sigma_{\min}/\sigma_{\max} \geq 0.2$
Circular Probable Error	50%	$CPE = 1.1774 \sigma_c$ $CPE = 0.5887 (\sigma_x + \sigma_y)$ when $\sigma_{\min}/\sigma_{\max} \geq 0.2$ $CPE \sim (0.2141 \sigma_{\min} + 0.6621 \sigma_{\max})$ when $0.1 \leq \sigma_{\min}/\sigma_{\max} \leq 0.2$ $CPE \sim (0.0900 \sigma_{\min} + 0.6745 \sigma_{\max})$ when $0.0 \leq \sigma_{\min}/\sigma_{\max} \leq 0.1$
Circular Map Accuracy Standard	90%	$CMAS = 2.1460 \sigma_c$ $CMAS = 1.0730 (\sigma_x + \sigma_y)$ when $\sigma_{\min}/\sigma_{\max} \geq 0.2$
Circular Near-Certainty Error (Three-five sigma)	99.78%	$3.5000 \sigma_c$

semi-major and semi-minor axes  $\sigma_a$  and  $\sigma_b$ . Applying the assumptions of the previous section on  $d_{rms}$  to this case,  $\sigma_c$  for the concentric range-azimuth case is given by equation 2.22.

$$\sigma_c = 0.5000 \left( \sigma_r + \frac{r \sigma_\theta}{57.296} \right) \quad (2.22)$$

### C. THE ERROR OF AN INTERPOLATED FIX

The error in an interpolated position for both methods of interpolation used in range-azimuth positioning will now be derived. Fundamental to the derivation is an understanding of the concept of error propagation, which is explained in detail in Greenwalt (1962) and Davis (1981). Error propagation is summarized here for the special case of range-azimuth positioning. It must be noted that any interpolation discussed in this chapter is strictly due to errors in the observed positions between which the interpolation is made. Error due to the vessel not being at its interpolated position (due to steering or wind and sea conditions) will be considered in later chapters.

#### 1. Interpolation Algorithms

The present NOS methods of interpolating range-azimuth fixes are of two types. One interpolates both the range and angle between two observed positions. The second is used when actual range information is acquired on each sounding. In this case only the angle is interpolated, and is used with the observed range to compute a position. In each case a linear interpolation is used [Ehrhardt, 1979]. Algorithms for the interpolated value of the range,  $r_i$ , and the angle  $\theta_i$ , are given in equations 2.23 and 2.24.

$$r_i = r_1 + (j/K+1)(r_2-r_1) \quad (2.23)$$

$$\theta_i = \theta_1 + (j/K+1)(\theta_2-\theta_1) \quad (2.24)$$

where:

Subscript i denotes interpolated.

Subscript 1 denotes observed position number 1.



Subscript 2 denotes observed position number 2.

K denotes the number of interpolations.

j steps from one to K.

The following example of the interpolation process is also sketched in figure 2.8.

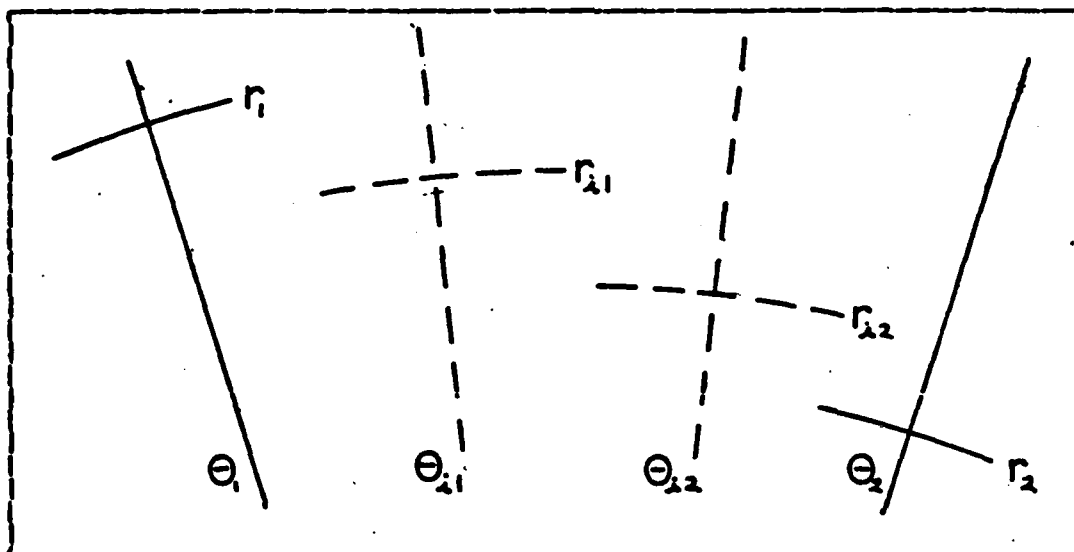


Figure 2.8 Example of Angular Interpolation.

Let:  $\theta_1 = 251^\circ$      $r_1 = 1501m$      $j = 1 \text{ to } 2$   
 $\theta_2 = 244^\circ$      $r_2 = 1485m$      $K = 2$

The values of the interpolated angles and ranges are computed by equations 2.24 and 2.23.

$$\theta_{11} = 251 + (1/3) (244-251) = 251 - 2.3 = 248.7^\circ \quad (2.25)$$

$$\theta_{12} = 251 + (2/3) (244-251) = 251 - 4.6 = 246.4^\circ \quad (2.26)$$

$$r_{\lambda 1} = 1501 + (1/3) (1485-1501) = 1501-5.3 = 1495.7m \quad (2.27)$$

$$r_{\lambda 2} = 1501 + (2/3) (1485-1501) = 1501-10.7 = 1490.3m \quad (2.28)$$

## 2. Error Propagation

"Error propagation is better termed the propagation of variances and covariances" [Davis, 1981]. The following paragraphs are a general derivation of error propagation, and will be applied below. In reading this section, the terms  $x$  and  $y$  are general, yet the reader should remember that they will be applied specifically to range-azimuth interpolation. Let  $y$  be a set of quantities each of which is a function of another set of random variables  $x$ . The random variables in our application are the observed  $x$  given in equation 2.1, and  $y$  is the interpolated  $\theta_i$  or  $r_i$  given in equations 2.24 or 2.23.

The covariance matrix  $\sum_{yy}$  is given by the matrix equation 2.29, where  $J_{yx}$  is called the Jacobian matrix and is given in equation 2.30.

$$\sum_{yy} = J_{yx} \sum_{xx} J_{yx}^T \quad (2.29)$$

$$J_{yx} = \begin{bmatrix} \frac{\partial y_1}{\partial x_1} & \frac{\partial y_1}{\partial x_2} & \frac{\partial y_1}{\partial x_3} & \cdots & \frac{\partial y_1}{\partial x_N} \\ \frac{\partial y_2}{\partial x_1} & \frac{\partial y_2}{\partial x_2} & \frac{\partial y_2}{\partial x_3} & & \vdots \\ \frac{\partial y_3}{\partial x_1} & \frac{\partial y_3}{\partial x_2} & & & \vdots \\ \vdots & \vdots & & & \vdots \\ \frac{\partial y_N}{\partial x_1} & \cdots & \cdots & \cdots & \frac{\partial y_N}{\partial x_N} \end{bmatrix} \quad (2.30)$$

$J_{yx}^T$  is the transpose of  $J_{yx}$ , and  $\Sigma_{xx}$  is another covariance matrix given by :

$$\Sigma_{xx} = \begin{bmatrix} \sigma_1^2 & \sigma_{12}^2 & \sigma_{13}^2 & \dots & \sigma_{1N}^2 \\ \sigma_{12}^2 & \sigma_2^2 & \sigma_{23}^2 & & \\ \sigma_{13}^2 & \sigma_{23}^2 & \sigma_3^2 & & \\ \vdots & & & \ddots & \\ \sigma_{1N}^2 & \dots & \dots & \dots & \sigma_N^2 \end{bmatrix} \quad (2.31)$$

The covariance matrix in equation 2.31 is written for the general case of correlated random variables. If  $y$  is a single quantity rather than a set of quantities, and if the variables are assumed uncorrelated, equation 2.29 reduces to:

$$\sigma_y^2 = \begin{bmatrix} \frac{\partial y}{\partial x_1} & \frac{\partial y}{\partial x_2} & \dots & \frac{\partial y}{\partial x_N} \end{bmatrix} \begin{bmatrix} \sigma_1^2 & & & \\ & \sigma_2^2 & & \\ & & \sigma_3^2 & \\ & & & \ddots \\ & & & & \sigma_N^2 \end{bmatrix} \begin{bmatrix} \frac{\partial y}{\partial x_1} \\ \frac{\partial y}{\partial x_2} \\ \vdots \\ \frac{\partial y}{\partial x_N} \end{bmatrix} \quad (2.32)$$

By carrying out the multiplication in equation 2.32, the expanded form is given in equation 2.33.

$$\sigma_y^2 = \left( \frac{\partial y}{\partial x_1} \right)^2 \sigma_1^2 + \left( \frac{\partial y}{\partial x_2} \right)^2 \sigma_2^2 + \dots + \left( \frac{\partial y}{\partial x_N} \right)^2 \sigma_N^2 \quad (2.33)$$

If  $y$  is a linear function of random variables, the partial derivative terms in equation 2.33 become constants. Thus the matrix equation 2.29 becomes equation 2.34, where  $a, b, c$ , and  $d$  are constants.

$$\sigma_y^2 = a^2 \sigma_1^2 + b^2 \sigma_2^2 + c^2 \sigma_3^2 + \dots + d^2 \sigma_N^2 \quad (2.34)$$

Now let us apply equation 2.34 to the range-azimuth case. The assumptions made above are:

- (i)  $y$  is a single quantity
- (ii) The random variables  $x$  are assumed uncorrelated.
- (iii)  $y$  is a linear function of  $x$

If these are applied to the two interpolation algorithms, equations 2.24 and 2.23, it can be seen that:

- (i)  $\theta_i$  and  $r_i$  are single quantities.
- (ii) The random variables  $\theta_1$ ,  $\theta_2$  and  $r_1$ ,  $r_2$  are assumed uncorrelated.
- (iii) The two interpolation algorithms are linear.

From the foregoing general discussion the interpolated variances of equations 2.23 and 2.24 can be given as:

$$\sigma_{r_i}^2 = \sigma_{r_1}^2 + \left( \frac{j}{K+1} \right) (\sigma_{r_2}^2 - \sigma_{r_1}^2) \quad (2.35)$$

$$\sigma_{\theta_i}^2 = \sigma_{\theta_1}^2 + \left( \frac{j}{K+1} \right) (\sigma_{\theta_2}^2 - \sigma_{\theta_1}^2) \quad (2.36)$$

but,

$$\sigma_{r_1}^2 = \sigma_{r_2}^2 = \sigma_r^2 \quad (2.37)$$

and:

$$\sigma_{\theta 1}^2 = \sigma_{\theta 2}^2 = \sigma_{\theta}^2 \quad (2.38)$$

By substituting equations 2.37 and 2.38 into equations 2.35 and 2.36, we have:

$$\sigma_{r_i}^2 = \sigma_r^2 \quad (2.39)$$

and

$$\sigma_{\theta i}^2 = \sigma_{\theta}^2 \quad (2.40)$$

This error propagation applies only to vessels moving in an arc. For a vessel moving in a straight line the angular interpolation algorithm is not linear and the partial derivative terms analogous to those in equation 2.33 are not constants. The error ellipse for an interpolated position can now be formed. The ellipse is seen to be the same as for an observed position (figure 2.5) since equations 2.39 and 2.40 show that errors in interpolated distance and angle are the same as for an observed distance and angle.

### III. EXPERIMENT DESIGN AND IMPLEMENTATION

The experimental work performed in this investigation can be conceptually divided into two parts, although both parts were accomplished simultaneously. Part one involved pointing error and variance determination for the two theodolites, and part two investigated the accuracy of interpolated positions.

#### A. FIELD WORK

The actual field work was representative of a typical range-azimuth survey. Two full days (8 and 15 April, 1983) were required to obtain 443 position fixes and over 2500 Aztrac angles. The experiment took place in southern Monterey Bay near the Monterey Harbor Coast Guard Pier, as shown in Figure 3.1. The vessel used was a chartered 36-foot Uniflite with a fiberglass hull and twin engines, and its operator had about two months' hydrographic survey experience, including steering range arcs.

For each position of the vessel, six lines of position were observed. Three Wild T-2 theodolites located at stations MUSSEL, SOFAR, and USE MON were used to obtain the "reference" or best estimate positions of the vessel. Two additional test theodolites, a Wild T-2 and an Odom Aztrac, made observations from stations T2 and AZTRAC. Finally, a Del Norte Trisponder (model R04) provided a distance LOP to the vessel from station GEOCEIVER. The reference positions were obtained at one minute intervals, and five Aztrac angles were observed between each of these positions for later use in evaluating interpolation methods. Figure 3.2 shows the sources of the various LOP's to the vessel. It

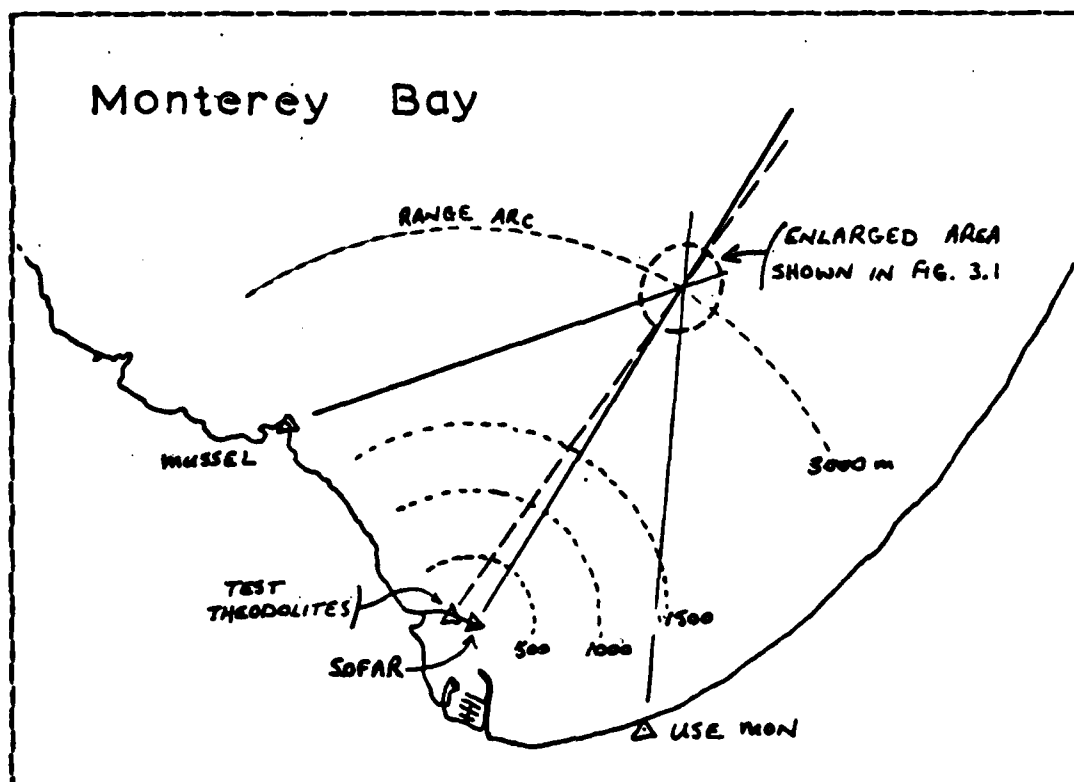


Figure 3.1 Sketch of the Survey Area.

represents an enlargement of the dashed circle area shown in Figure 3.1.

Geodetic control for the reference positions consisted entirely of monumented third-order stations. Station GEOCEIVER, although not a published station, was located to third order specifications by Mr. William Anderson of NAVOCEANO in 1982, and the other two stations were located as eccentrics of this station. Each was less than one meter from GEOCEIVER. GEOCEIVER is a monumented station, while Aztrac and T2 are marked by masonry nails driven into the concrete pier. Positions for Aztrac and T2 were computed on an HP-9815 computer using the NGS geodetic direct program. The initial pointing by both instruments was to station USE

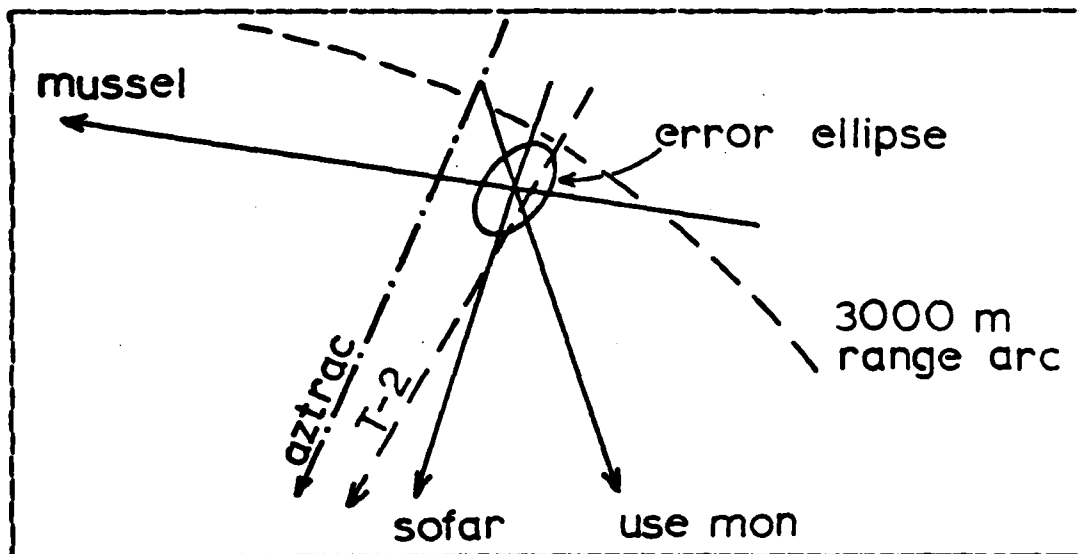


Figure 3.2 Lines of Position Observed to the Vessel.

MON. Initial pointings at all stations were made to third-order stations at least 500 meters distant. Geodetic positions of all control stations is given in Appendix B.

Underway operations were very similar to a nonautomated range-azimuth survey, except that five theodolites, rather than one, were trained on the boat for each fix. The survey boat steered along the appropriate range arc, and fix marks were given over voice radio to the observers on shore. All T-2 angles were obtained once each minute, and Aztrac angles were recorded every ten seconds. The sequence of events for each reference position is given in Table II.

This process continued throughout the two-day field operation. Breaks in data collection occurred at the ends of each range arc, and also when theodolite observers were rotated. The monotony of the events shown in Table II was sufficient to approximate the monotony (with its associated observer difficulties) of an actual survey.



**TABLE II**  
**Data Acquisition Sequence of Events**

time prior to fix	action
20 sec	depress Aztrac manual fix button
15 sec	"15 second standby" over voice radio
10 sec	depress Aztrac manual fix button
5 sec	"standby" over voice radio
0 sec	"mark" over voice radio, depress Aztrac manual fix button, T-2 operators make observations

Observers at stations MUSSEL and USE MON were required to record angles as well as to observe. T-2 observers at stations T2 and SOPAR were provided with separate recorders, because at times the high angular speeds of the vessel at these stations (due to closeness of the boat) made observing and recording difficult for one person.

The Trisponder was calibrated using the standard NOS method over a geodetic baseline (GEOCEIVER to USE MON) and no systematic errors were observed. The geodetic baseline was determined by computing an inverse distance between stations USE MON and GEOCEIVER using the HP9815 computer and NGS geodetic software. The Trisponder was reported by Odom Offshore Surveys to have a standard deviation of its ranging error of 1.0 meters. The master unit and antenna were mounted at the highest part of the boat, about one meter above and aft of a radar antenna enclosure, which was about one meter in diameter and 0.4 meter high. The master unit was a cube about 0.3 meter on a side and was covered with

green signal cloth. This unit was the target to which angles were observed. The Trisponder Distance Measuring Unit (DMU) was mounted next to the steering station inside the boat.

Data logging for both Trisponder and Aztrac was accomplished by an Odom Navtrace computer system. Both the Trisponder DMU and Aztrac receiver were interfaced to this unit. The Navtrace computer is programmed to automatically log fix data not on intervals of equal time, but on equal distance intervals from a reference line. For this reason, all fixes were logged by using the manual fix feature of the computer. This simply caused the computer to log distance and angle each time a button was manually pressed. Timing for fixes was provided by an NOS standard sounding clock. This is a mechanical clock with a buzzer set to ring every ten seconds.

The weather during both days of field work was good to fair for survey work. Visibility was good at all times, and winds were calm on each morning of operations. Afternoon northwest winds were a maximum of about 15 knots on both days, which produced two to three foot seas in the offshore part of the operating area.

#### B. THEODOLITE POINTING ERROR

The pointing error,  $x_i$ , is defined as the difference between an observed and computed angle given by

$$x_i = \theta_o - \theta_c \quad (3.1)$$

and the mean pointing error,  $\bar{X}$ , is therefore

$$\bar{X} = \frac{1}{n} \sum_{i=1}^n x_i \quad (3.2)$$

where  $n$  is the number of observations,  $\theta_o$  is the observed azimuth and  $\theta_c$  is the computed azimuth from the theodolite position to the reference position of the vessel. The standard deviation,  $\sigma_\theta$ , of a set of pointing errors can be expressed mathematically as

$$\sigma_\theta = \sqrt{\frac{1}{n-1} \sum_{i=1}^n (\bar{x} - x_i)^2} \quad (3.3)$$

This is the usual definition in most statistics texts and agrees with the discussion in section II.A. of this paper.

The computed azimuth,  $\theta_c$ , was determined by computing a geodetic forward azimuth from either test theodolite position to the reference position of the vessel. There is some potential error in  $\theta_c$  due to an uncertainty in the reference position of the vessel. The reference position of the vessel was determined by a least squares adjustment of the three LOP's from the three Wild T-2 theodolites. A by-product of this adjustment is an error ellipse for each position. The angle subtending this error ellipse from each test theodolite is the error in  $\theta_c$ . This is illustrated in Figure 3.3.

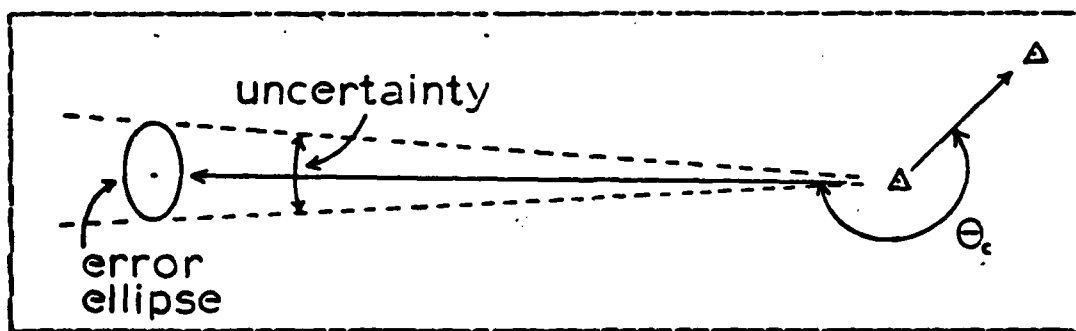


Figure 3.3 Uncertainty of an Observed Error.

The least squares method was developed in 1794 by Gauss. It is based on the concept that as soon as redundant observations are present there appear discrepancies among the observations. In order to eliminate these discrepancies a residual,  $v$ , must be added to each observation. In the method of least squares the residuals are determined such that the sum of their squares becomes a minimum, provided all observations have the same accuracy [Mueller, 1979]. It is assumed that the three LOP's used in this adjustment do in fact have the same accuracy. Further information on the method of least squares as applied to hydrography is given by Kaplan (1980).

Reference positions were calculated by the least-squares FORTRAN program AZLSQ2, written by the author, which is a modification of program SILVA1 [Silva, 1979]. The program generated plane and geodetic coordinates for each position fix, as well as the lengths of the semi-major and semi-minor axes of its error ellipse. The angle made by the semi-major axis and the x-axis was also computed.

### C. INTERPOLATION ALGORITHM EVALUATION

The present NOS method of observing azimuths to the sounding vessel is totally nonautomated, as explained in section A. This precludes recording an azimuth for each sounding because of the speed with which soundings are taken. Consequently interpolation algorithms are employed to plot soundings between observed positions. Two algorithms are used: one interpolates only the azimuth and uses an observed distance to the vessel, while the other interpolates both azimuth and distance. Figures 3.4 and 3.5 illustrate the situation.

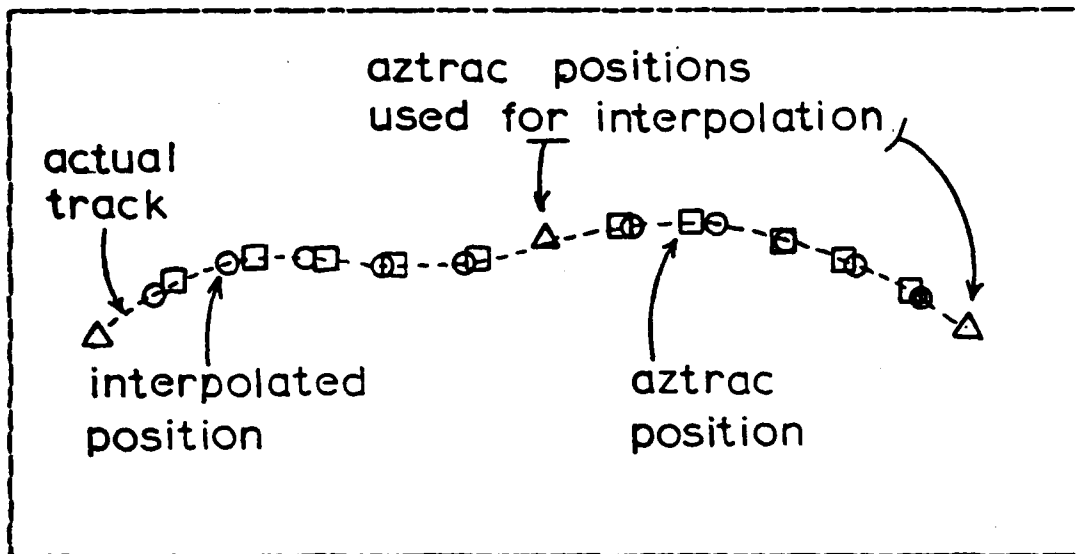


Figure 3.4 Interpolation of Angle Only.

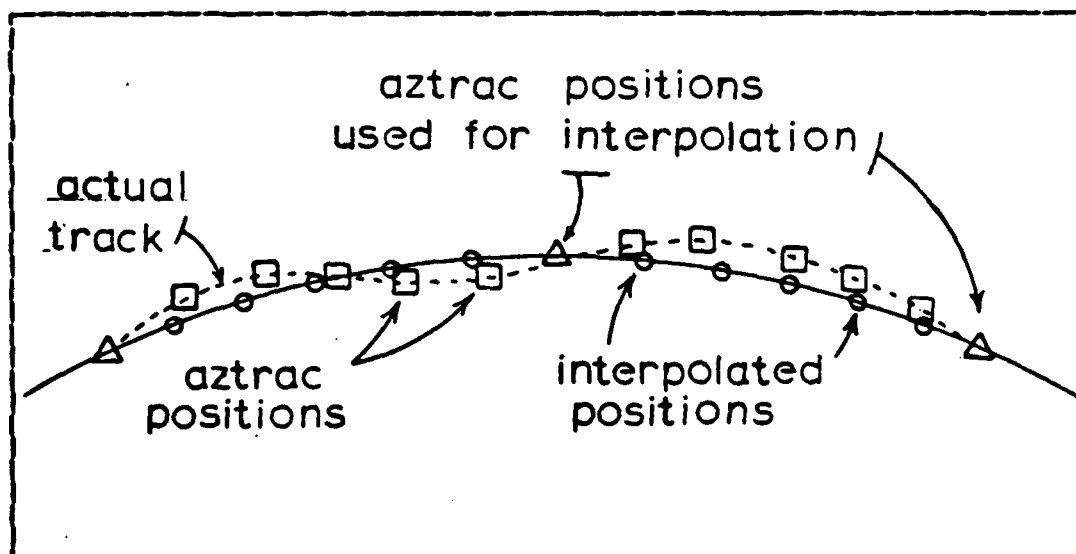


Figure 3.5 Interpolation of Angle and Distance.

The method used to evaluate these interpolation methods is simple. Actual distances and angles to the vessel were

recorded every ten seconds, using the telemetering theodolite and associated computer logging system. A nonautomated system was then simulated by interpolating between positions obtained every minute. Thus two data sets were produced, an interpolated set and a corresponding set of actually observed positions. These two sets of positions were then compared and their differences examined. Both NOS interpolation algorithms were evaluated in this manner. An analysis of the experimental results is given in Chapter IV.

#### D. CHOICE OF EXPERIMENTAL CONDITIONS

Any experiment must be performed under conditions similar to those under which the results will be applied. This section will describe the specific error sources to be examined under range-azimuth conditions. By carefully choosing the experimental conditions, these error sources can be brought into the foreground for examination, while all other sources of error can be kept in the background.

It is necessary to introduce some standard statistical terminology to help understand the experiment design. The classical experimental method studies the effect of only one variable. That is, it holds all effects but one to be constant, and varies that single one systematically. In the case of this thesis, one factor (a theodolite) was varied systematically by introducing two levels (Aztrac and T-2) of the factor. It is desired to find the effect of that factor (the theodolite) on the error of a range-azimuth position. It is known, however, that the observer also has a considerable effect on the error of a position. Thus another factor (the observer) is introduced into the experiment. Four levels (four different individual observers) of this factor were selected.

The following four observers, who are attached to the Naval Postgraduate School, constitute the four levels of the observer factor.

LCDR Gerald B. Mills, NOAA. Instructor in Hydrography. Ten years experience in geodetic and hydrographic surveying.

LT Maureen Kenny, NOAA. Student in hydrography. 2 years field experience aboard the NOAA Ship Davidson, primarily in Alaskan and West Coast waters.

LT Mary C. Schomaker, NOAA. Student in hydrography. 4 years field experience aboard NOAA Ship Davidson, and on NGS horizontal control and leveling parties.

Mr. James R. Cherry, Supervisory Geodesist, Naval Postgraduate School. 23 years field experience in hydrography and geodesy, with the Naval Oceanographic Office.

Although additional observers would have been desired, none were available who had any experience with theodolites.

Aside from the factors to be investigated, it was recognized that there were background conditions that affected the results of the experiment [Crow, 1955]. Some of these were taken into account explicitly in the design. The influence of all others was minimized by scheduling the experiment such that each combination of instrument and observer was evaluated in random order, thereby randomizing the effects of these other conditions.

Blunders and some systematic errors were explicitly accounted for in the design. Blunders were identified visually by their large magnitude and were simply deleted from the data set using the editor on the NPS computer. The Aztrac instrument essentially eliminates all blunders due to its automatic data logging feature.

Systematic errors integral to the theodolites, such as collimation and eccentricity, were not accounted for, since they were very small compared to the size of the errors under investigation. One systematic error that could be quite large is the initial pointing error, which is due largely to the observer. The NOS Hydrographic Manual [Umbach, 1976] requires the initial pointing to be "accurate to within  $\pm 30$  seconds of arc". That is, the difference between beginning and ending pointings is not to exceed one minute. For this experiment, the mean of the beginning and ending pointings to the initial azimuth was algebraically subtracted from all observed angles for that set. It could be argued that a more accurate way of removing this systematic error would be to prorate the difference in initial readings between the beginning and ending pointings. However, the former method is often used by NOS hydrographic survey units.

One background condition, the angular speed of the vessel, was explicitly taken into account in the design by dividing the experiment into groups. Six separate subsets of the experiment were created by measuring pointing error at six different angular speeds. These speeds were chosen to be closely representative of speeds found under actual surveying conditions. To this end, integral values of angular speed were not used, but rather integral distances from the vessel to the theodolite station. This corresponds to actual practice in most nonautomated or semiautomated surveys. The vessel maintains constant engine speed, and is



navigated in a circle such that a constant distance value is displayed in the ranging equipment. For this experiment, distances of 300, 500, 700, 1000, 1500, 3000 meters were used. Using the approximate vessel speed of 2 meters per second (4 knots), the angular speeds in minutes per second corresponding to these distances were 22.9, 13.8, 9.8, 6.9, 4.6, and 2.3, respectively.

Another background condition that was explicitly accounted for in the design was the experience of the observers. For a completely general investigation, one would desire to evaluate the error using observers of widely varying experience. Only experienced observers were used in order to conserve resources of time and money, although none of them were experienced in using the new Aztrac instrument. All observers except LCDR Mills had acted as observer for range-azimuth hydrography within the past year using the Wild T-2.

There were other background conditions that affected the results of the experiment, including weather and lighting conditions, and observer fatigue. Other subtle factors may have also contributed to the error. In nonautomated systems, there might have been a time lag by the radio operator in the vessel as the fix mark was relayed to the theodolite operator ashore. The design of the experiment could not explicitly account for all these conditions, so several steps were taken to randomize the order of observations for each combination of instrument and observer.

It was assumed that the theodolites used were randomly drawn from the entire population of T-2 and Aztrac instruments. This is a fairly good assumption for the T-2, since the particular unit tested is one of several maintained by the Naval Postgraduate School, and has seen several years of service. The assumption for the Aztrac theodolite is not as good, since it is one of only five in existence at this time. It was provided by the manufacturer for testing.

Theodolite observers were required to be paired, since the experimental theodolites observed simultaneous angles to the vessel. A random selection of observer pairs was accomplished by consulting a random number table in Wonnacott (1977). The order of observation for the six different range arcs was important and required randomization. Failure to do so could allow the error associated with each to be influenced by time varying conditions. Examples of these are the changing effect of sun glare on the instrument, observer fatigue, the effect of repetition acting to decrease error, or increasing afternoon winds disturbing the theodolite. Randomization was again accomplished with the aid of a random number table. A random number was assigned to each range arc, and the order of observation was established by selecting the arcs from the lowest to highest number.

## **IV. RESULTS AND DATA ANALYSIS**

### **A. DATA PROCESSING SYSTEM**

All data acquired for this experiment were manually entered into the NPS computer facility. A data processing system was designed and implemented to log the raw data and perform the necessary computations to arrive at the finished form given in this chapter. This system was divided into numerous subsystems to enter data, determine the pointing error, compute interpolated positions, compute means and variances, test for randomness, and compute analysis of variance (ANOVA) statistics. ANOVA is a standard statistical technique used in testing for a difference between the effects of two or more factors.

The data processing system was designed and programmed by the author. As mentioned previously, the NGS geodetic inverse and direct subroutines [Pfaifer, 1975], as well as the least-squares adjustment program [Silva, 1979], were adapted for use here. The ANOVA computations were performed by the Statistical Package for Social Sciences (SPSS) on the Naval Postgraduate School mainframe computer [Hull, 1981]. The pointing error and interpolation subsystems were designed as described in Chapter III.

### **B. POINTING ERROR DETERMINATION**

The pointing error standard deviation for each theodolite needs to be quantified, and a determination must be made as to whether there is a statistically significant difference between the two instruments. Pointing error for each combination of instrument and observer was determined by the methods discussed in Chapter III. Standard deviation

of the pointing error was computed using equation 3.3, for each combination of instrument and observer, at each range arc, and are given in Appendix A. This entire procedure was performed first for the T-2 angles observed to the nearest second of arc, which is the maximum resolution for this instrument, and second, for T-2 angles rounded to the nearest minute of arc, which is specifically allowed by the NOS Hydrographic Manual [Umbach, 1976].

Since eight different instrument-observer combinations exist, the sample means and standard deviations for each combination were slightly different because each sample is only an estimate of the mean, , and standard deviation, , for the entire population. The pooled standard deviation is the best estimate of for this case of multiple samples because it takes the differences among sample means into account. If an overall standard deviation is computed using equation 3.3, the population standard deviation will be overestimated because of the differences among sample means. The pooled standard deviation is mathematically expressed by equation 4.1 [Crow, 1955], [Box, 1978].

$$s_o = \sqrt{\frac{(n_1-1)s_1^2 + (n_2-1)s_2^2 + \dots + (n_k-1)s_k^2}{n_1 + n_2 + \dots + n_k - k}} \quad (4.1)$$

where:

- k = total number of observer-instrument combinations
- n = number of observations for each observer-instrument combination
- s = sample variance for each observer-instrument combination

Thus a pooled standard deviation was computed for the eight samples available at each different range arc. These are

given in Table III for the Aztrac and both the rounded and unrounded T-2 data. This table gives angular speeds for the vessel in units of minutes of arc per seconds of time. Note that the pointing error of the Aztrac is twice as large as that of the T-2 and that the rounded T-2 pointing error is only slightly greater than the unrounded.

**TABLE III**  
**Pointing Error Standard Deviation (pooled estimates)**

Range Arc (m)	Approx. Angular Speed (min/sec)	Aztrac		T-2 (unrounded)		T-2 (rounded)	
		m (sec)		m (sec)		m (sec)	
		$\sigma_a$	$\sigma_o$	$\sigma_a$	$\sigma_o$	$\sigma_a$	$\sigma_o$
300	22.9	3.33	(2290)	1.26	(868)	1.31	(902)
500	13.8	3.56	(1470)	1.72	(712)	1.73	(715)
700	9.8	2.10	(619)	1.30	(382)	1.31	(386)
1000	6.9	2.97	(613)	1.08	(225)	1.09	(226)
1500	4.6	4.25	(584)	0.92	(126)	0.93	(128)
3000	2.3	2.06	(142)	1.41	(97)	1.43	(99)

The technique of analysis of variance (ANOVA) is used to determine whether a statistically significant difference exists between the two theodolites. The ANOVA technique allows the partitioning of overall pointing error variance into portions caused by each factor (observer and theodolite), by interaction, and by experimental error. Interaction exists if the variance for a particular combination of instrument and observer is greater than the variance for any other such combination. The experimental error is

primarily due to the conditions described in Chapter III, concerning the reference positions for the vessel. This error is a measure of the precision of the experiment, where precision is defined as the closeness with which repeated measurements made under similar conditions are grouped together [Greenwalt, 1971]. Experimental error is assumed to have a population mean of zero. Further details of the ANOVA method can be found in many statistics textbooks, such as Wonnacott (1977), Box (1978), Crow (1955), and Walpole (1978). This discussion was taken primarily from Crow (1955).

The following assumptions must be made when using the analysis of variance technique.

- (i) Observations are random.
- (ii) Means and variances are additive, as given in the mathematical model below.
- (iii) Experimental errors are independent.
- (iv) Variances of the experimental errors are equal.
- (v) Distribution of the experimental errors is normal.

A mathematical model can now be given, using these assumptions, which specifies the total effects of the variances acting on a particular observation,  $x_{ij}$ .

$$x_{ij} = \mu + a_i + b_j + \delta_{ij} + e_{ij} \quad (4.2)$$

where:

$\mu$  = overall mean for all observations

$a_i$  = effect of the instrument factor at level  $i$

$b_j$  = effect of the observer factor at level  $j$

$\delta_{ij}$  = effect of the interaction of instrument and observer at level  $i$  and  $j$ , respectively.

$e_{ijt}$  = random effect caused by the variance of the experimental error.

$i = 1, 2$

$j = 1, 2, 3, 4$

$t = 1, 2, 3, \dots, n$

$n$  = the number of observations for a particular observer-instrument combination (usually 15)

It should be emphasized that the  $a$ ,  $b$ ,  $\delta$ , and  $e$  of equation 4.2 are not actual variances, but a realization of the effect of those variances on a particular observation  $x_{ijt}$ . The variances associated with observer, instrument, and interaction are computed by the ANOVA procedure, and these form the basis of the test for differences. This test is called the F-test in honor of Sir Ronald A. Fisher [Wonnacott, 1977], and is based on a ratio of variances. To test for a difference between instruments, we form a ratio with the variance among instruments in the numerator, and a denominator composed of an estimate of the variance of the experimental error. In terms of our mathematical model,  $a$  (the numerator) is being compared with  $e_{ijt}$  (the denominator). More simply stated, it is a comparison of the precision of the instrument (the numerator), with the precision of the experiment (the denominator). This ratio,  $F$ , is then compared to a ratio  $F_\alpha$ , which is computed for a particular confidence level from the F-distribution function given as equation 4.3 [Crow, 1955].

$$P(F) = \int_F^{\infty} \frac{\left(\frac{f_1 + f_2 - 2}{2}\right)!}{\left(\frac{f_1 - 2}{2}\right)! \left(\frac{f_2 - 2}{2}\right)!} f_1^{f_1/2} f_2^{f_2/2} F^{(f_1 - 2)/2} (f_2 + f_1 F)^{-(f_1 + f_2)/2} dF \quad (4.3)$$

where:  $F$  = the ratio discussed above

$f_1$  = the number of degrees of freedom  
in the numerator of  $F$

$f_2$  = the number of degrees of freedom  
in the denominator of  $F$

A precise hypothesis must now be stated that can be tested by the  $F$ -test. Walpole (1974) states that "a statistical hypothesis is an assumption or statement, which may or may not be true, concerning one or more populations." Experiments are designed to test hypotheses, and "the rejection of an hypothesis is to conclude that it is false, while acceptance merely implies that we have no reason to believe otherwise" [Walpole, 1978]. A null hypothesis is an "initial hypothesis, or one we hope to reject" [Crow, 1955], and is usually stated in terms of an assumption of no difference between the effects to be investigated by the experiment. This experiment uses three null hypotheses, which are:

- (i) There is no difference between observers, that is, the ratio  $F$ , for observers, is small compared to  $F_{\alpha}$ .
- (ii) There is no difference between instruments, that is, the ratio  $F$ , for instruments, is small compared to  $F_{\alpha}$ .
- (iii) There is no interaction, that is, the ratio  $F$  for interaction, is small compared to  $F_{\alpha}$ .



These three null hypotheses can be accepted or rejected on the basis of the F-test and the ANOVA procedure. If any are to be rejected, the value of the ratio F must exceed that of the critical  $F_{\alpha}$  for that confidence level (95%). A summary of ANOVA results is given in Table IV. For each range arc, the computed values of F and the corresponding critical value needed to reject the null hypothesis are given. The rightmost column of the areas labelled as rounded or unrounded data indicate acceptance or rejection of the null hypothesis. It can be seen from this table that in no case could the null hypothesis be rejected for either instrument or observer. In other words, it may be said with 95% confidence that there is no reason to believe there is a difference between the four observers or between the two instruments. It should be noted that data for the 1500 meter arc indicate a rejection of the null hypothesis for interaction. According to Crow (1955), a significant interaction usually occurs because unrandomized background conditions are present. There is little apparent reason why this interaction should occur, other than that there were some unidentified, time varying conditions affecting the measurements. The 1500 and the 1000 meter range arc were only observed on April 8, while all the other range arcs were investigated on both days of the experiment.

A final assumption of the ANOVA technique is that the observations within the eight combinations of instrument and observer are randomly drawn from their populations. Several tests are available to determine if a particular sample is random. The test used here was the Run Test, as given in Crow (1955), and a confidence level of 95% was used. This test showed all eight samples were random at the 95% confidence level.

**TABLE IV**  
**Summary of ANOVA Results at 95% Confidence**

	$F_{\alpha}$	Rounded Data		Unrounded Data	
		F	null hyp.	F	null hyp.
<b>300 m arc</b>					
instrument	3.97	0.10	accept	0.09	accept
observer	2.70	1.69	accept	1.69	accept
interaction	2.70	1.36	accept	1.35	accept
<b>500 m arc</b>					
instrument	3.92	0.01	accept	0.01	accept
observer	2.68	0.13	accept	0.14	accept
interaction	2.68	0.25	accept	0.25	accept
<b>700 m arc</b>					
instrument	3.84	0.05	accept	0.05	accept
observer	2.60	1.86	accept	1.86	accept
interaction	2.60	0.28	accept	0.29	accept
<b>1000 m arc</b>					
instrument	3.92	0.01	accept	0.01	accept
observer	2.68	0.45	accept	0.45	accept
interaction	2.68	1.74	accept	1.79	accept
<b>1500 m arc</b>					
instrument	3.84	0.78	accept	0.73	accept
observer	2.68	1.44	accept	1.41	accept
interaction	2.68	5.01	reject	5.02	reject
<b>3000 m arc</b>					
instrument	3.95	0.10	accept	0.12	accept
observer	2.70	1.69	accept	1.74	accept
interaction	2.70	1.36	accept	1.37	accept

### C. INTERPOLATION EVALUATION

The two methods of interpolation used by NOS were next evaluated. As explained in section III.C., three sets of positions were computed. These were a set of actually observed positions using Aztrac, and two sets of corresponding positions computed by the two different interpolation algorithms discussed in section II.C. These two algorithms were evaluated by computing the distance between each observed position and each corresponding interpolated position. A FORTRAN program written by the author performed the computations. The NGS geodetic direct subroutine [Pfeifer, 1975] was used to compute positions from observed distances and Aztrac directions to the vessel. The interpolated positions were computed using equations 2.23 and 2.24, which are the same algorithms used in the NOS interpolation subroutine TCARC [Ehrhardt, 1979]. Distances between the two corresponding positions were computed on a plane, rather than using a geodetic computation. There is negligible difference between plane and geodetic methods at the distances (about ten meters) under consideration here. Results of these computations are given in Table V, which shows for each range arc the average distance in meters separating the interpolated and the corresponding observed positions. An indication of the variability of these values is shown by the percentage of interpolated positions falling farther than 1.0 meter away from the actual position.

Little can be inferred from the results in Table V because this table is really an intermediate step towards a rigorous evaluation of the raw data. This table should be viewed as only a general indication of the effectiveness of interpolation. Since it is a direct result of the ability of the boat operator to steer the vessel in an arc, wind and sea conditions have a tremendous effect on interpolation

**TABLE V**  
**Results of Interpolation Evaluation**

Range n	Angle Only		Angle and Distance	
	$\bar{Y}$	% > 1.0 m from mean	$\bar{Y}$	% > 1.0 m from mean
3000	1.15	47%	2.41	55%
1500	2.09	85%	4.98	91%
1000	1.63	72%	4.07	78%
700	2.04	75%	3.01	80%
500	1.86	79%	4.15	83%
300	2.59	79%	5.32	84%

effectiveness. Although this experiment was carried out in representative survey conditions, Table V should not be viewed as being applicable to all situations. The table does indicate that, whenever possible, automatic recording of range data should be used.

Full analysis of the interpolation algorithms should be the two-dimensional equivalent of testing for the difference between means. This is because both the interpolated and observed positions are not "true" positions, but have some error. A one-dimensional test of differences between means is well established, and is discussed in several references, including Wonnacott (1977). The null hypothesis for such a test is

$$d = \mu_1 - \mu_2 \quad (4.4)$$

where  $\mu_1$  and  $\mu_2$  are the means of the two populations, and  $d$  is some arbitrary distance selected by the experimenter. The two-dimensional problem has the same null hypothesis but the mathematics of the test have not been established. This problem is illustrated in Figures 4.1 and 4.2.

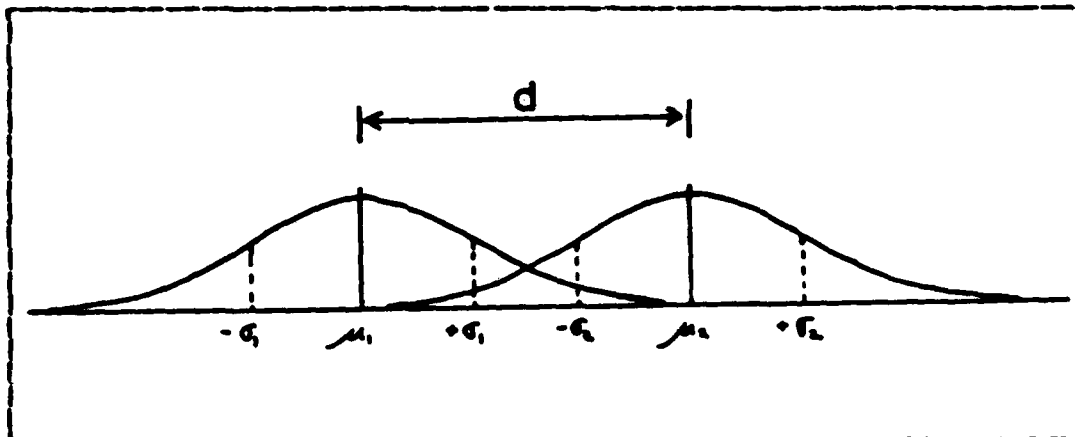


Figure 4.1 One-Dimensional Difference Between Means.

A proper analysis of the data would inquire for each interpolated-observed pair of positions, whether the distance between the two positions was greater than  $d$  for a particular confidence. More work than could be incorporated into this thesis is required to fully evaluate the data.

#### D. ANALYSIS OF FACTORS AFFECTING THE RESULTS

The results of this experiment were presented in Tables III, IV, and V. An attempt will now be made to analyze the experiment for errors in logic and technique, in order to better understand these findings.

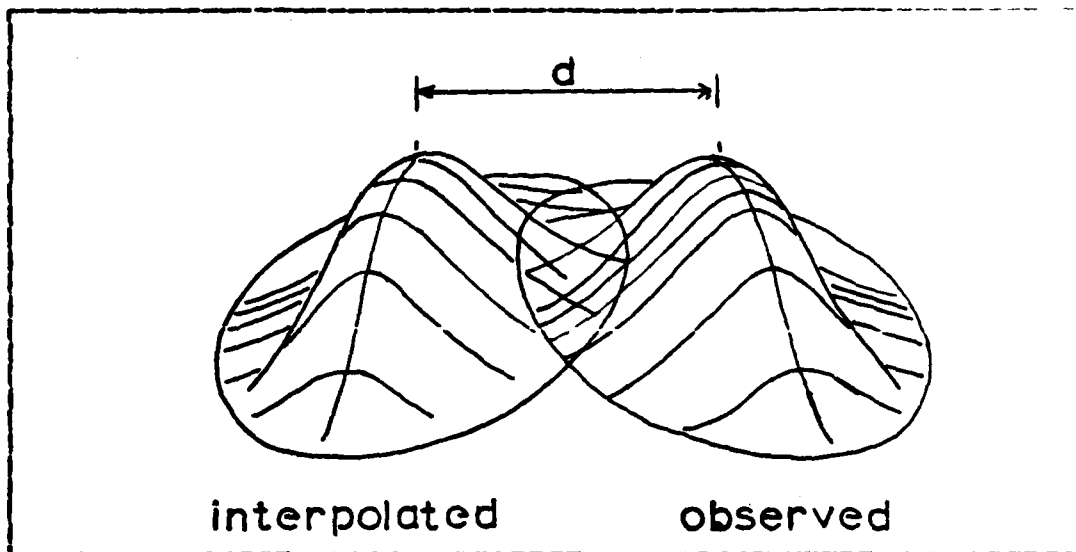


Figure 4.2 Two-Dimensional Difference Between Means.

The most important results from this thesis are the estimates of  $\sigma$  for theodolite pointing error. It is obvious from Table III that standard deviations of both the rounded and unrounded T-2 error values are about one-half that of the Aztrac, for all angular speeds considered. The ANOVA technique, however, shows no statistical difference between the instruments at the 95% confidence level. An analysis of the data used to obtain the results yields a potential explanation for this apparent contradiction.

The original data (pointing errors in seconds of arc) were made the subject of empirical probability density plots using the subroutine HISTG [Robinson, 1974] on the NPS computer. These plots show probability density versus error, as well as mean and standard deviation. An example of these plots, for the 500 meter range arc, is given in Figure 4.3. The remaining plots are found in Appendix C. Plots are shown for both Aztrac and T-2 (unrounded), for each range arc. A striking feature of the Aztrac curves is

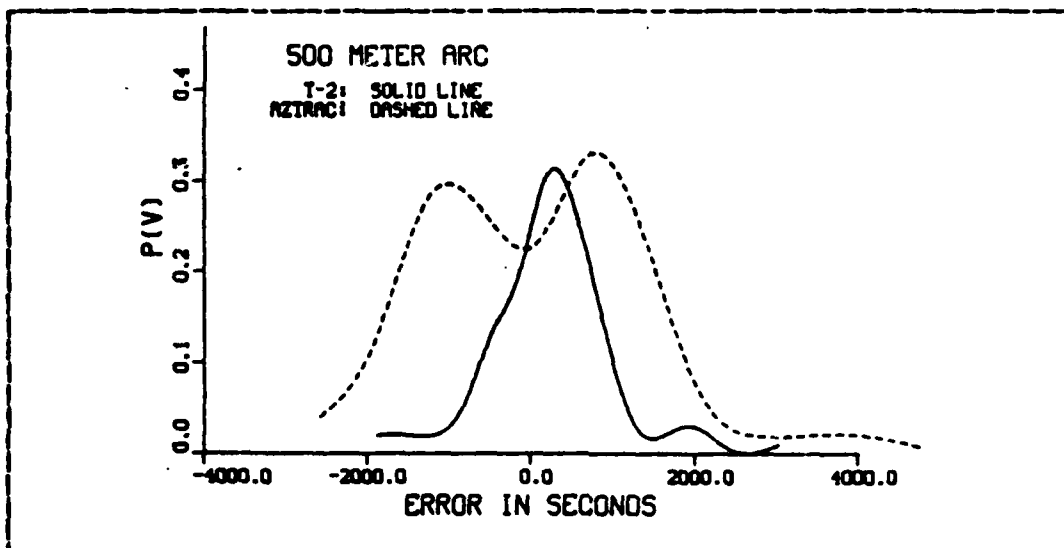


Figure 4.3 Probability Density vs. Error.

their bimodal shape, as compared to a single peak for the T-2 curves. It can be easily seen from the curves how the spread of this bimodal distribution would increase the computed standard deviation for the Aztrac data.

The method of data acquisition for this thesis was semiautomated in that all T-2 angles were manually recorded, while the Aztrac angles were recorded by pressing a button aboard the vessel. It is probable that a time lag existed between all the T-2 observations and the Aztrac observations, despite the best efforts of the observers, because the observation procedure was not totally automated. If this were true, there would be little difference between the observed angle  $\theta$  for the T-2 and the computed angle  $\theta_c$ , because  $\theta_c$  is associated with a reference position also derived from T-2 observations. The observed angle  $\theta_o$  for the Aztrac would, however, be consistently different from  $\theta_c$  because of this time lag and because the vessel was moving to the left or right with respect to the Aztrac observer.

Since approximately equal numbers of observations were made with the boat moving to the left or right along the range arc, the distribution of Aztrac pointing errors would take on a bimodal shape.

It is understood that the data analyzed by these curves come from not one but four different samples, and that the curves should not be expected to be perfectly peaked. The T-2 curves, however, also come from four samples and do not have multiple peaks. This analysis is further supported by finding the distance between one peak of the Aztrac curve and the single peak of the T-2 curve in figure 4.3. The distance in arc seconds, when converted to meters, is roughly the distance the vessel traveled in one second. One second of time is certainly a reasonable figure for the time lag discussed above. A manual check of the raw data recorded in the field also suggests such a time lag. The original data were sorted into two sets of "left" and "right" observations, which were analyzed for mean and standard deviation. Results of the analysis are shown in Table VI. This table gives the mean and standard deviation for the "left" and "right" data sets, and shows that the mean of both sets was about two meters to the left or right of the reference position of the vessel. This two meter difference corresponds closely to a nominal vessel speed of two meters per second (four knots) for the boat used, and a time lag of one second. Means for the 1500 and 3000 meter ranges are somewhat unequal because sea conditions at these offshore ranges caused the boat to travel slower in one direction. The rightmost column in Table VI gives the pooled standard deviation of each "left" and "right" data set, which is the best estimate of the population standard deviation,  $\sigma_0$ , for the Aztrac.



TABLE VI  
Corrected Aztrac Standard Deviation

Arc	left/ right	Mean, $\bar{X}$	s	Aztrac Pooled Standard Deviation
		n (sec)	n (sec)	
300	L	2.95 ( 2035)	1.17 ( 806)	1.07 (741)
	R	-2.67 (-1836)	0.99 (682)	
500	L	2.40 ( 993)	1.50 (660)	1.44 (598)
	R	-2.69 (-1112)	1.31 (539)	
700	L	1.61 ( 476)	0.90 (266)	1.05 (312)
	R	-2.37 ( -700)	1.28 (379)	
1000	L	2.49 ( 514)	1.55 (321)	1.43 (296)
	R	-2.92 (-604)	1.30 (268)	
1500	L	1.93 (266)	1.56 (228)	1.45 (199)
	R	-3.22 (-444)	1.06 (147)	
3000	L	0.48 (33)	1.42 (98)	1.30 (90)
	R	-3.97 (-273)	1.22 (84)	

The systematic error caused by a time lag as the boat moved left or right in the observer's field of view was the result of faulty design of the experiment. The proper way to correct this problem would be to duplicate the experiment using better synchronization of all observations. An alternative would be to model the systematic error and apply corrections to the existing data. Such a model should include an estimate of the boat speed and its left or right direction with respect to the observer.

Different ANOVA results might be obtained using the data corrected for systematic error, but this would not explain the ANOVA results in Table IV. The conditions affecting data acquisition must again be considered, as well as an

understanding of the ANOVA process, when offering an explanation.

The denominator of the F-ratio discussed in section B is essentially the experimental error of the measurement process. This error is primarily a function of the error ellipse for the "reference" position shown in Figure 3.3. Table VII gives an estimation of this experimental error, by comparing the size of the error in  $\theta_o$  and  $\theta_c$ . Uncertainty in  $\theta_c$  is given as the mean major axis of all error ellipses for a given range arc. Uncertainty in  $\theta_o$  is the pooled standard deviation,  $\sigma_o$ , of each test theodolite. The values for  $\sigma_o$  in the Aztrac column are from Table VI, and the T-2 values are from Table III. An examination of Figure 3.3 shows that use of the major axis of the ellipse is a worst case estimate of the uncertainty, since the ellipse could have any orientation in the x-y plane. Thus it can be seen from Table VII that the uncertainty in  $\theta_c$  is smaller than that of the observed azimuth  $\theta_o$ . This comparison is an indicator of the precision of the experiment.

If this error in the computed angle,  $\theta_c$ , could be reduced by decreasing the size of the error ellipse, the denominator of the F-ratio would be smaller and the ratio itself would be larger. Thus a more precise experiment could produce a rejection of the null hypothesis, although this is not indicated in light of the values of  $\sigma_o$  for the Aztrac and T-2 shown in Table VII. Reducing experimental error any further than this study would be difficult under typical hydrographic conditions, because the three LOP theodolite intersection position, adjusted by the least-squares method, is one of the most precise positioning means available today. The size of the reference position error ellipse could possibly have been reduced if better intersection angles were available, but this was not possible with the particular geographic shape of Monterey Bay.

TABLE VII

## Experiment Precision and Rheodolite Error

Range, meters	Mean major axis meters (sec)	Aztrac pooled std. deviation meters (sec)		T-2 pooled std. dev. meters (sec)	
		$\sigma_1$	$\sigma_0$	$\sigma_1$	$\sigma_0$
300	.974 (668)	1.07	(741)	1.26	(868)
500	.838 (344)	1.44	(598)	1.72	(712)
700	.754 (222)	1.05	(312)	1.30	(382)
1000	.824 (170)	1.43	(296)	1.08	(225)
1500	.738 (102)	1.45	(199)	0.92	(126)
3000	1.188 (82)	1.30	(90)	1.41	(97)

In summary, the analysis of variance performed on these data do, in fact, show that there is no statistical difference between Aztrac and T-2 at 95% confidence. This procedure is a strictly numerical one and must be viewed in light of the original research conditions. When these conditions are carefully analyzed to remove as much systematic error as possible, the data strongly suggest that the ANOVA results are indeed correct.

## E. APPLICATION TO POSITION ERROR STANDARDS

From Chapter I it can be seen that there is some confusion in the hydrographic community as to the application of probability to positioning standards. With this in mind, there appear to be four possibilities for consideration as standards with which to compare the results of this thesis, as given below.

- (i) The 1968 IHO standard of 1.5 m at the

survey scale, with the 90% probability suggested by Munson (1977).

- (ii) The 1982 IHO standard of 1.0 mm at the scale of the survey, with 90% probability.
- (iii) The current range-azimuth standard of NOS (0.5 mm at the survey scale) assuming a probability associated with  $d_{rms}$ .
- (iv) The  $d_{rms}$  standard of microwave range-range positioning found in Umbach (1976). This requires that  $d_{rms}$  values at the survey scale not exceed 0.5 mm for 1:20,000 scale surveys and smaller, 1.0 mm for 1:10,000 scale surveys, and 1.5 mm for surveys of 1:5,000 scale and larger.

These four possibilities may now be compared to the position errors of the Aztrac and T-2 by using the pointing error results given in Table VII. Since the precision of a range-azimuth position is also a function of the standard deviation of ranging error,  $\sigma_r$ , assumed values of 1.0 and 3.0 meters are used in this analysis. Some manufacturers of microwave ranging equipment used in range-azimuth positioning report a 1.0 meter value for  $\sigma_r$ , but 3.0 meters is most often used by NOS personnel [Wallace, 1983] and has some supporting experimental evidence by unbiased experimenters [Munson, 1977].

Using these assumed values for  $\sigma_r$  and the observed values for  $\sigma_2$  given in Table VII, the error ellipse axes may be computed using equations 2.11 and 2.12. However, the error ellipse must be converted to a circular error figure in order to be compared with the standards above. The assumed standards (i) and (ii) must use a 90% probability circle, which can be computed using Table I, and standards

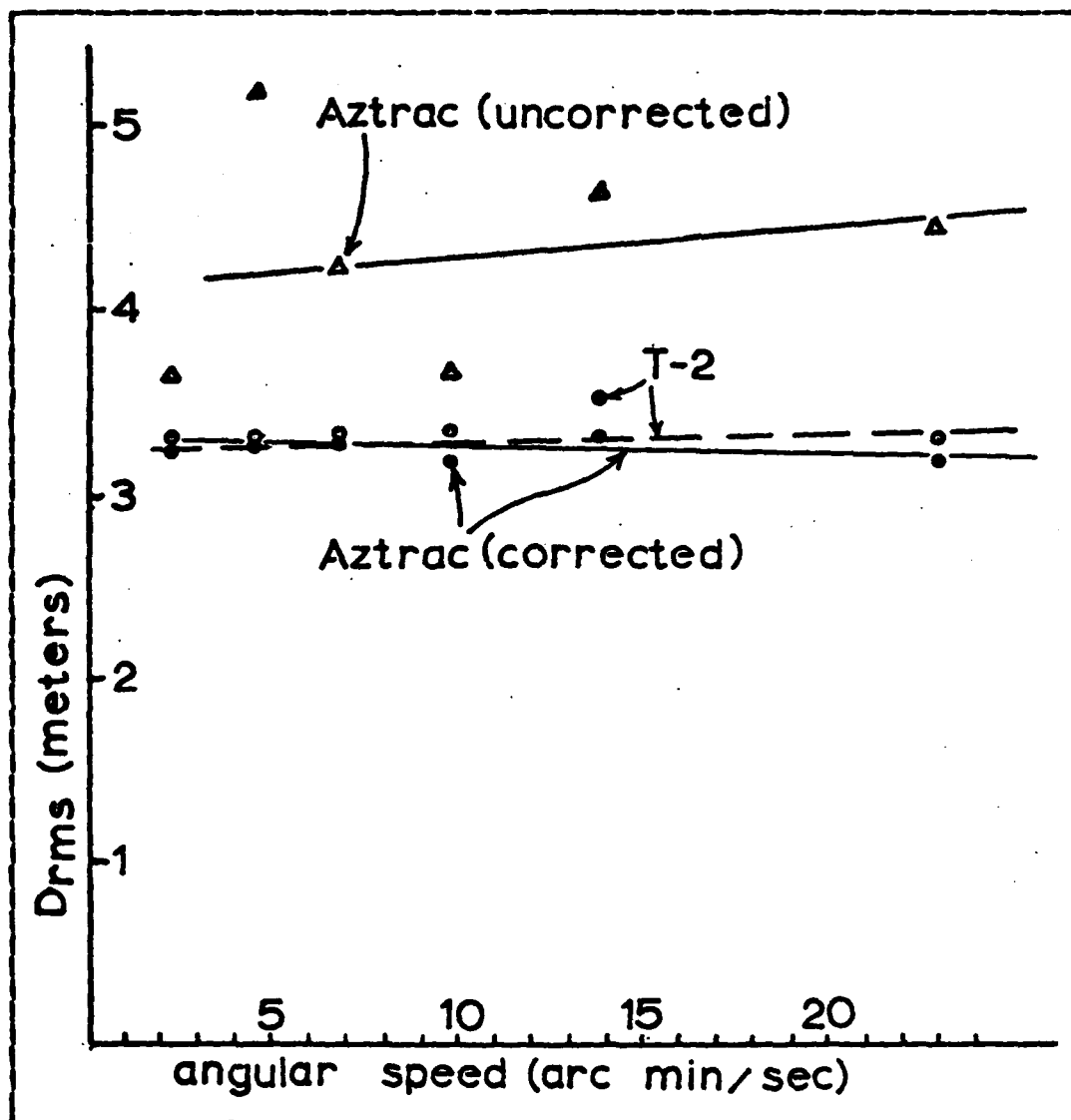


Figure 4.4 Results Compared to  $d_{rms}$ .

(iii) and (iv) must use the  $d_{rms}$  formula given by equation 2.16. Results of these computations are shown graphically in Figure 4.5 for 90% probability, and in Figure 4.4 for  $d_{rms}$ . Each figure has angular speed of the theodolite along the abscissa, and an ordinate consisting of a distance scale, in meters, indicating the radius of the error circle.

The error circle for Figure 4.5 is associated with the 90% probability level, while the  $d_{rms}$  circle for Figure 4.4 is of somewhat variable probability, as discussed in Chapter II. The points plotted in Figure 4.5 have eccentricity values ( $\sigma_z/\sigma_r$ ) ranging from 0.3 to 0.6, which indicate a probability range of from about 65% to 67.5%.

These figures also clearly show an improvement in the estimate of  $\sigma_\theta$  for the Aztrac as a result of the time lag correction discussed earlier. The position error values for the uncorrected Aztrac error is shown by triangles in both figures, while position error computed using the corrected  $\sigma_\theta$  values are shown by solid dots. For both Aztrac cases, two solid linear regression lines are drawn. Both figures show that the uncorrected Aztrac values have a much greater variability than the corrected values, and that the corrected values are almost the same as the T-2 position error values indicated by open dots and dashed linear regression lines. If the corrected Aztrac values are taken to be the best estimate of position error for this instrument, then a relatively constant error is indicated for the entire range of angular speeds considered here. This is about 3.3 meters  $d_{rms}$  and 4.6 meters (90% probability) for both instruments using a  $\sigma_r$  value of 3.0 meters, and 1.6 meters  $d_{rms}$  and 2.5 meters (90%) for a  $\sigma_r$  value of 1.0 meters. Plots are not shown for computations using a range error of 1.0 meter.

The four possible assumptions for position error standards are compared to Aztrac and T-2 position errors in Table VIII. The roman numerals heading the columns of this table refer to the position standards associated with the same numerals at the beginning of this section. The reader should use the table by selecting one of these columns and inspecting it from the top to the bottom of the table. The first row of Table VIII indicates the probability associated

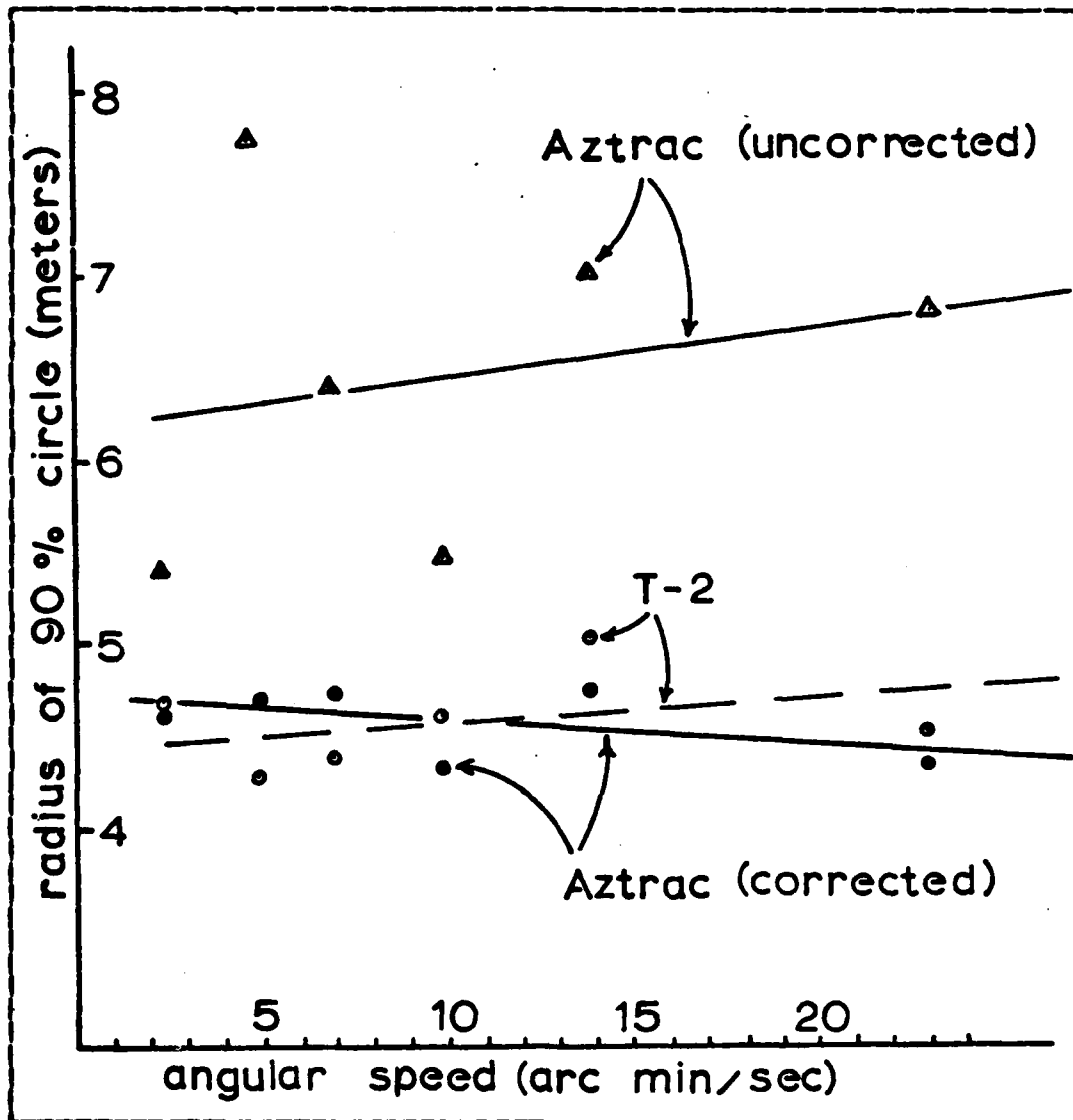


Figure 4.5 Results Compared to 90% Probability.

with each positioning standard. The second row lists the maximum position error allowed by that standard, at the scale of the survey. Rows three and four show the errors allowed in row two, when converted to actual distances for two representative survey scales of 1:5,000 and 1:10,000. Rows five and six show the radius of the associated

probability circle for both Aztrac and T-2, for ranging error values of 3.0 and 1.0 meters, respectively. The dual probability percentages in columns (iii) and (iv) indicate the variable probability of  $d_{rm}$ . Dual values in column (iii) for maximum error at the survey scale result from the NOS standard for range-range positioning. The remainder of the table presents conclusions as to whether the T-2 and Aztrac meet the various standards. For example, in column (iv) the observed 3.3 meter  $d_{rm}$  value in row five is less than the maximum allowable error of 5.0 meters shown in row four. Therefore, the T-2 and Aztrac do meet the NOS range-azimuth standards of 0.5 mm at the scale of the survey for 1:10,000 scale surveys.



**TABLE VIII**  
**Position Standards Comparison**

	(i) IHO (1968)	(ii) IHO (1982)	(iii) NOS (r/r)	(iv) NOS (r/a)
Assumed Probability	90%	90%	68%- -63%	68%- -63%
Allowable Max Error at Scale	1.5 mm	1.0 mm	1.5, 1.0 mm	0.5 mm
Allowable Max Error at 1:5,000	7.5 m	5.0 m	7.5 m	2.5 m
Allowable Max Error at 1:10,000	15.0 m	10.0 m	10.0 m	5.0 m
Aztrac & T-2 Error ( $\sigma_1 = 3.0m$ )	4.6 m	4.6 m	3.3 m	3.3 m
Aztrac & T-2 Error ( $\sigma_1 = 1.0m$ )	2.5 m	2.5 m	1.6 m	1.6 m

Conclusion As To Meeting Standards:  $\sigma_1 = 3.0 m$

	(i)	(ii)	(iii)	(iv)
1:5,000 scale	yes	yes	yes	no
1:10,000 scale	yes	yes	yes	yes

Conclusion As To Meeting Standards:  $\sigma_1 = 1.0 m$

	(i)	(ii)	(iii)	(iv)
1:5,000 scale	yes	yes	yes	yes
1:10,000 scale	yes	yes	yes	yes

## V. CONCLUSIONS AND RECOMMENDATIONS

Of the original objectives for this thesis discussed in Chapter I, the first and most basic was the determination of pointing error standard deviation for the Aztrac and T-2 theodolites. No investigation of this type had ever been done for conditions typical of a range-azimuth survey. An experiment was carefully designed to determine this pointing error and to determine if there was a statistically significant difference between the instruments. The initial estimates of pointing error were given in Table III, which shows the Aztrac to have an error, when converted to distance, of about 3.0 meters, while the estimate was about 1.3 meters for the T-2.

An uncompensated systematic error in the data, due to the time lag discussed in Chapter III, was discovered when empirical probability density function plots were made of the entire data set for each instrument. This led to a revised estimate of the pointing error for the Aztrac, because the bimodal distribution caused by this time lag adversely affected the original estimate for  $\sigma_0$ . This revised estimate is about 1.3 meters, as shown in Table VII, and is almost the same as the value of  $\sigma_0$  for the T-2 instrument. When these estimates for  $\sigma_0$  are viewed in light of the precision of the experiment, as shown in the table, it is seen that the actual values of  $\sigma_0$  could be smaller than indicated, because smaller values would be masked by the relative imprecision of the experiment. It is to be concluded, however, that the actual values of the pointing error of each instrument are no larger than those given here.

The question of a statistically significant difference between the instruments was then considered using the ANOVA technique, which can be said to compare a variance component due to the instruments with a variance component due to the precision of the experiment. This precision was not very much greater than the variance of the instruments, but was based on the most precise positioning method generally available for hydrography -- an intersection position using three theodolites. The ANOVA procedure indicated no significant difference between instruments, but if the precision of the experiment had been increased, a significant difference could possibly have been detected. In light of the subsequent discovery and elimination of the systematic error due to a time lag, this conclusion of no difference between theodolites appears to be well justified.

An evaluation of interpolation methods was the second objective of this thesis, and although the analysis was not as rigorous as it could be, it can be concluded that there is a measurable distance between an interpolated position and a corresponding observed position. This has never been done for the case of range-azimuth positioning because the rapid position fixing available with Aztrac has not been available. It has been shown, through an error propagation analysis of the interpolation algorithms, that the interpolated error is not inherently due to the algorithms themselves. The error is therefore due to the inability of the vessel to follow the range arc, which is caused primarily because of environmental conditions and the vessel operator's track keeping capability. The distance between the interpolated and corresponding observed positions may be as much as two to four meters, as indicated in Table V, and is roughly twice as great for a position that is computed using both distance and angular interpolation, as for a position using angle interpolation alone. It is therefore

recommended that, whenever possible, automatic recording of range data should be used.

The third and most important objective of the thesis is a comparison of the total position error using these instruments with the required error standards of the major hydrographic survey organizations. The lower half of Table VIII gives these results, which are that all the standards considered are indeed met, except the NOS range-azimuth standard at 1:5,000 scale using a range error of 3.0 meters. This conclusion requires a very important qualification regarding the T-2 instrument and the errors encountered while pursuing the first two objectives. These are errors due to interpolation, and to the time lag discussed in Chapter IV.

The approximately one second time lag discovered with the Aztrac data set is not actually associated with the Aztrac at all but is associated with the T-2. It appeared to be a systematic error of the Aztrac in this experiment only because the reference positions were obtained using T-2 instruments similar to the test T-2. It must be concluded from the data acquired in this project that there exists, for any angle measured with a T-2, a time lag of about one second between angle observations and any measurement made aboard the vessel, including both automatic and manually recorded depth and range data. There is then an associated position error for these measurements, the magnitude of which depends upon vessel speed, which was about two meters for the four knot speed used in this experiment. The conclusions and position accuracies for observed T-2 positions in Table VIII do not take this additional error into account. When the error contributions from both the time lag and interpolation are considered, it can be concluded that positions interpolated between observed T-2 positions have an additional error of about two to four meters. Thus

the total actual position error for T-2 positions and positions interpolated between T-2 positions might fail to meet more of the standards than are indicated in Table VIII.

Having reached conclusions related to the objectives of the thesis, another set of conclusions and recommendations can be made for the Odom Aztrac theodolite, regarding its ease of use and suitability for range-azimuth hydrography. The Aztrac instrument was expressly designed for range-azimuth or azimuth-azimuth positioning, and has features which are advantageous to the operator of the instrument in the field. Such advantages are discussed in Chapter I, and include ease of tracking, because of an upright telescope image and an infinitely geared tangent screw.

The Aztrac theodolite possesses advantages much more important than ease of use in the field, and these additional advantages are derived primarily from its ability to be interfaced with a computer aboard the survey vessel. Besides eliminating systematic error due to a time lag, a computer based survey system offers the additional advantage of being able to measure and record a position every few seconds. This allows three important advantages over a system that can only measure positions once per minute. First, since each position is individually measured, no interpolation is required and thus better accuracy is obtained than with a nonautomated system. Second, no manual data logging is required, which reduces blunders and greatly increases the speed with which a survey may be processed. Third, an automated system allows the surveyor to run straight sounding lines rather than curved arcs, because an automated system can provide an almost real-time cross track error indication to the helmsman. Running straight sounding lines increases survey efficiency by orienting the lines more normal to the depth contours, and by requiring fewer total linear miles of hydrography for each survey. A vessel

may of course steer straight lines with a nonautomated system, but it is extremely difficult to maintain the strict line spacing requirements for hydrographic surveys without an indication of cross-track error, so curved range arcs are usually followed.

Disadvantages encountered during this experiment include additional operator fatigue caused by the requirement to constantly track the vessel. This is necessary if the substantially increased data rate available with this instrument is to be utilized. The extra effort to track the vessel is more than offset, however, by the elimination of manual data logging. Care is required by the operator when rotating the instrument through an arc, because if the instrument is moved too rapidly the maximum telemetry data rate is exceeded and erroneous angle data will be transmitted. This can only be detected by checking the original initial pointing. Although this problem was observed during a manufacturer's demonstration, it did not occur during the experimental field work. Finally, the transmitter range of 5 km is rather short for the distances used by NOS, which can be up to about 10 km. The manufacturer has stated that the system range can be easily extended by increasing the transmitter power [Apsey, 1983]. Although this thesis measured Aztrac error at a maximum distance of 3 km from the shore station, the conclusions stated here should not be blindly extrapolated to increased ranges. Still, if the Aztrac pointing error standard deviation is reduced to its angular resolution (0.01 degree) at the very slow angular speed of the vessel at long ranges, the error appears to remain acceptable. For example, 0.01 degree pointing error at a range of 10 km results in an error of only 1.74 meters.

The advantages of the Aztrac clearly outweigh its disadvantages, so it is therefore recommended that the Odom Aztrac system be incorporated into the computer based equip-

ment used by NOS. It should be used only in situations where it meets required positioning standards based on the value for  $\sigma_0$  found in this investigation. It is also recommended that the systematic error induced by the time lag discussed here should be accounted for in operational standards for range-azimuth positioning using the Wild T-2. This could be done for semi-automated systems by providing an automatic radio signal to the observer on shore that precedes the actual depth measurement by one second. A simpler method of reducing this systematic error could be a limit on the speed of the vessel, depending on the accuracy standard required for the particular survey.

A final recommendation must be made regarding the positioning standards of NOS. At present there are conflicting standards for a given survey scale, depending on whether electronic, hybrid (including range-azimuth), or visual methods are used. For example, positions for a 1:5,000 scale survey may be required to have an accuracy of either 7.5 meters  $d_{rms}$ , or 2.5 meters at some unspecified probability, depending on whether microwave range-range or range-azimuth methods are employed. The NOS is certainly the most progressive hydrographic organization with regard to position error specifications, but it is recommended that the concept of probability be applied to all positioning methods and not only electronic ones. Further, if the meaning of "seldom exceed" in the IHO standards is to be interpreted as a 90% probability circle, then all the NOS standards should be changed to reflect that standard.

# APPENDIX A

## MEANS AND STANDARD DEVIATIONS OF ACQUIRED DATA SETS

All values for means and standard deviations are in units of seconds of arc.

TABLE IX  
3000 Meter Arc

		Mills	Kenny	Schomaker	Cherry
Aztrac	X ==>	53	-306	68	-242
	s ==>	257	93	76	63
	overall mean =	-106	pooled s = 142		
T-2 un- rounded	X ==>	-34	29	113	-16
	s ==>	67	59	164	60
	overall mean =	23	pooled s = 97		
T-2 rounded	X ==>	-39	26	109	-10
	s ==>	75	62	163	57
	overall mean =	89	pooled s = 98		



TABLE X  
1500 Meter Arc

		Mills	Kenny	Schomaker	Cherry
Aztrac	X ==>	-124	476	37	-34
	s ==>	392	990	431	476
	overall mean =	88	pooled s = 584		
T-2 un- rounded	X ==>	27	-116	47	74
	s ==>	95	145	164	107
	overall mean =	8	pooled s = 126		
T-2 rounded	X ==>	32	-114	48	75
	s ==>	102	145	167	106
	overall mean =	11	pooled s = 128		

TABLE XI  
1000 Meter Arc

		Mills	Kenny	Schomaker	Cherry
Aztrac	X ==>	115	-116	-120	199
	s ==>	482	534	768	711
	overall	mean = 20      pooled s = 613			
T-2 un- rounded	X ==>	-45	17	125	-53
	s ==>	286	111	269	196
	overall	mean = 11      pooled s = 225			
T-2 rounded	X ==>	-49	13	133	-54
	s ==>	282	114	274	199
	overall	mean = 11      pooled s = 226			

TABLE XII  
700 Meter Arc

		Mills	Kenny	Schomaker	Cherry
Aztrac	X ==>	123	-114	36	208
	s ==>	585	777	508	542
	overall mean =	63	pooled s = 619		
T-2 un- rounded	X ==>	-14	-53	-55	156
	s ==>	307	338	210	681
	overall mean =	9	pooled s = 382		
T-2 rounded	X ==>	-14	-50	-60	160
	s ==>	311	342	205	690
	overall mean =	9	pooled s = 386		

TABLE XIII  
500 Meter Arc

		Mills	Kenny	Schomaker	Cherry
Aztrac	X ==>	284	4	98	-127
	s ==>	1543	1423	1957	930
	overall	mean = 65	pooled s = 1470		
T-2 un- rounded	X ==>	56	4	9	160
	s ==>	710	1037	452	618
	overall	mean = 57	pooled s = 712		
T-2 rounded	X ==>	62	0	15	163
	s ==>	710	1041	455	623
	overall	mean = 60	pooled s = 715		

TABLE XIV  
300 Meter Arc

		Mills	Kenny	Schomaker	Cherry
Aztrac	X ==>	425	-200	699	-1219
	s ==>	2274	1605	2104	3516
	overall mean =	-74	pooled s = 2290		
T-2 un- rounded	X ==>	-210	320	276	109
	s ==>	652	933	1290	682
	overall mean =	124	pooled s = 868		
T-2 rounded	X ==>	-215	313	274	43
	s ==>	654	929	1289	843
	overall mean =	104	pooled s = 902		

**APPENDIX B**  
**GEODETTIC POSITION OF HORIZONTAL CONTROL STATIONS**

Station Name	Latitude	Longitude
SOPAR (1947)	36 36' 32".117	121 53' 24".004
USE MON (1978)	36 36' 04".685	121 52' 35".900
MUSSEL (1932)	36 37' 18".151	121 54' 11".628
AZTRAC	36 36' 32".530	121 53' 25".310
T2	36 36' 32".493	121 53' 25".254
GEOCEIVER	36 36' 32".512	121 53' 25".286

**APPENDIX C**  
**EMPIRICAL PROBABILITY DENSITY FUNCTION PLOTS**

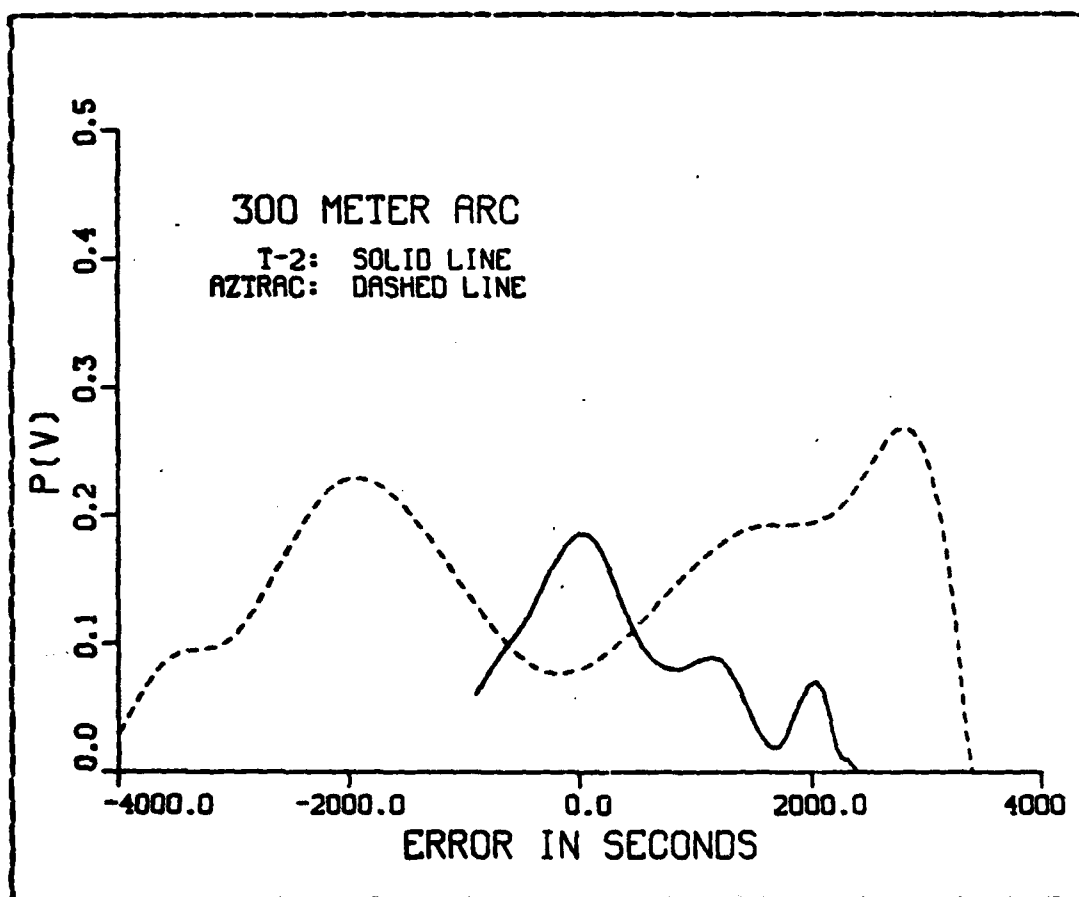


**Figure C.1 Probability Density Plot: 300 m arc.**

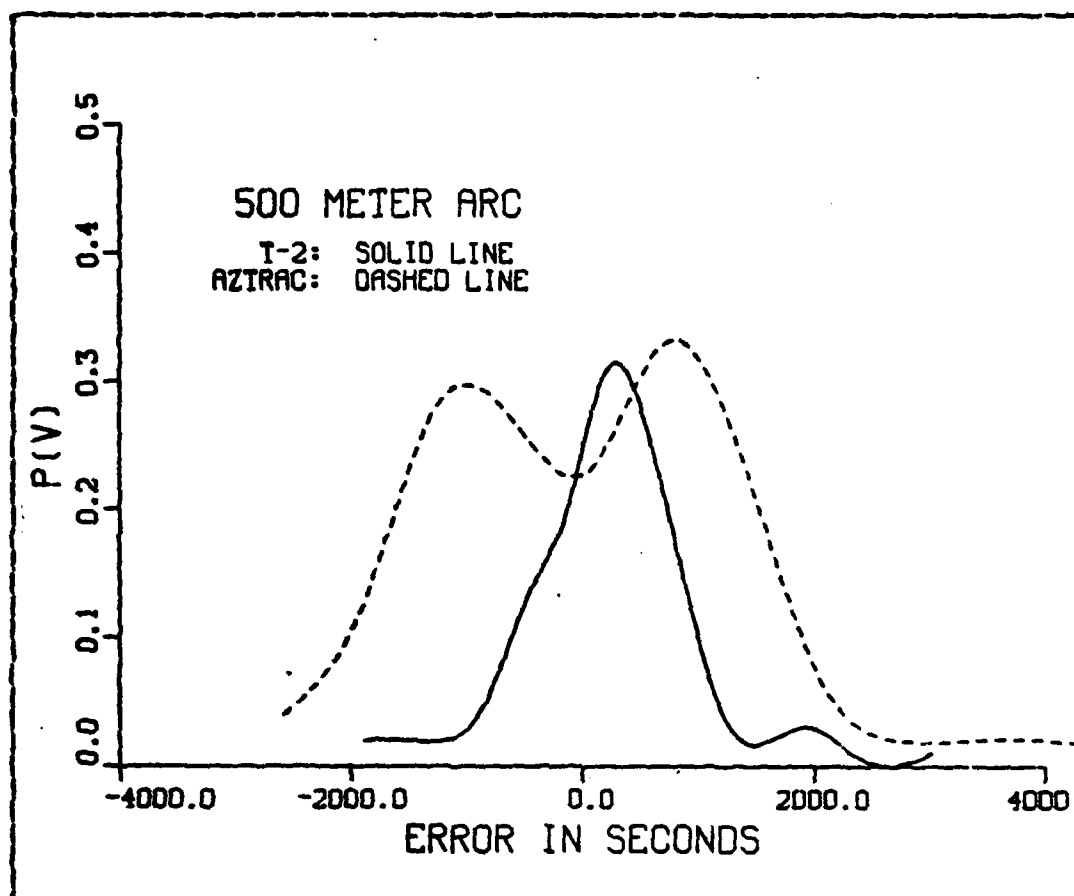


Figure C.2 Probability Density Plot: 500 m arc.



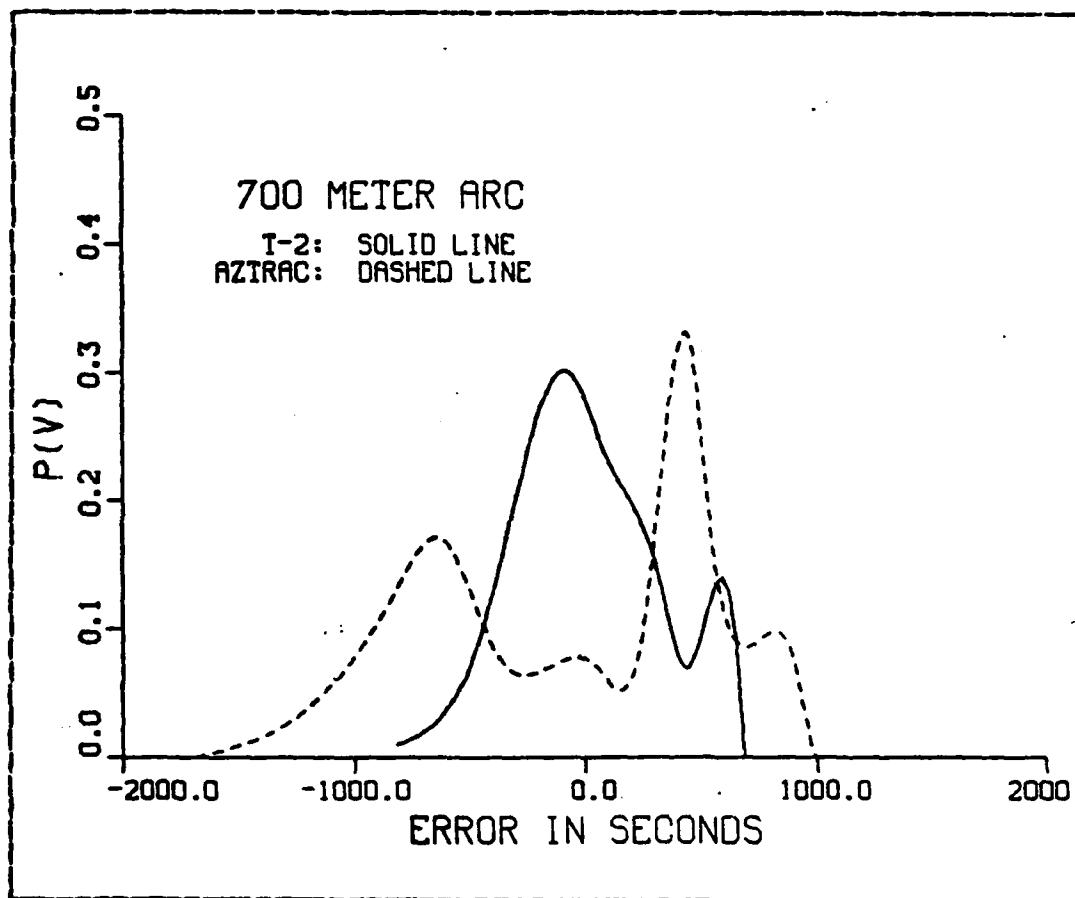


Figure C.3 Probability Density Plot: 700 m arc.

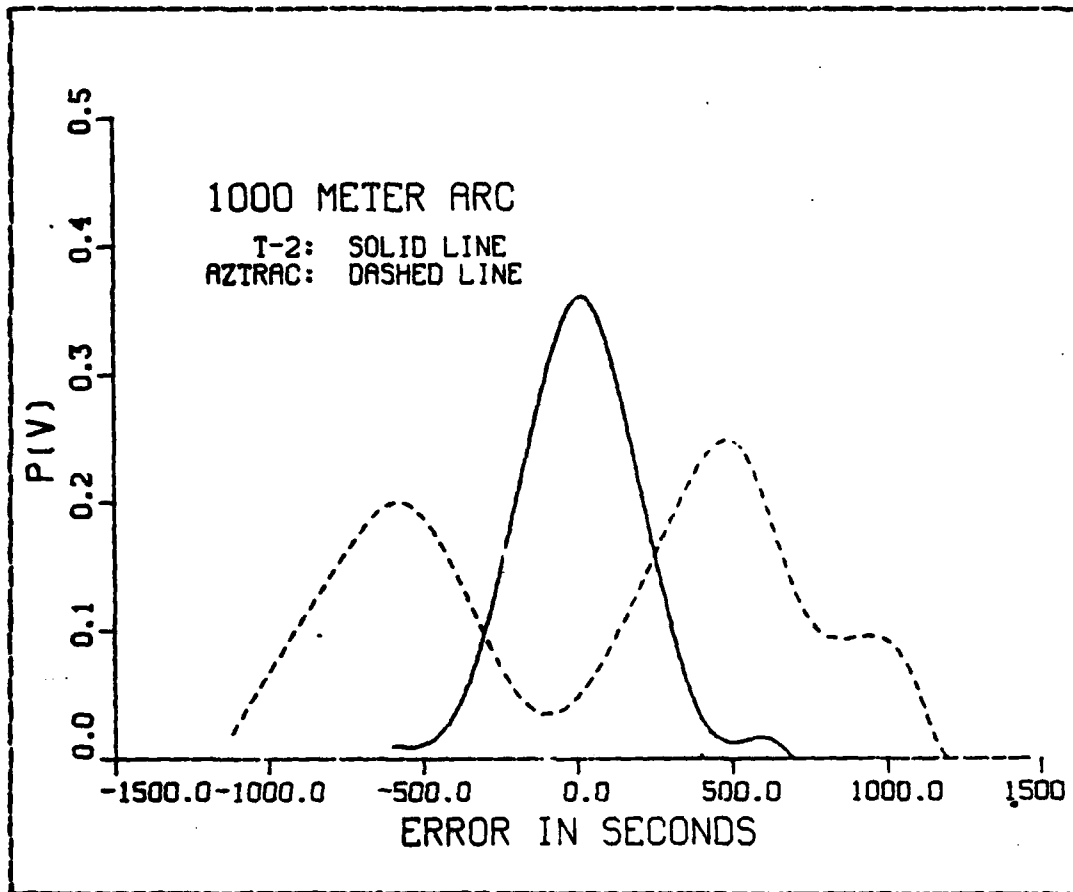


Figure C.4 Probability Density Plot: 1000 m arc.

AD-A136 775

AN ERROR ANALYSIS OF RANGE-AZIMUTH POSITIONING(U) NAVAL  
POSTGRADUATE SCHOOL MONTEREY CA D A WALTZ SEP 83

2/2

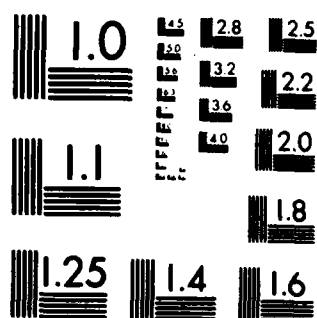
UNCLASSIFIED

F/G 8/2

NL



END  
DATE  
FILMED  
2 84  
DTIC



MICROCOPY RESOLUTION TEST CHART  
NATIONAL BUREAU OF STANDARDS-1963 A

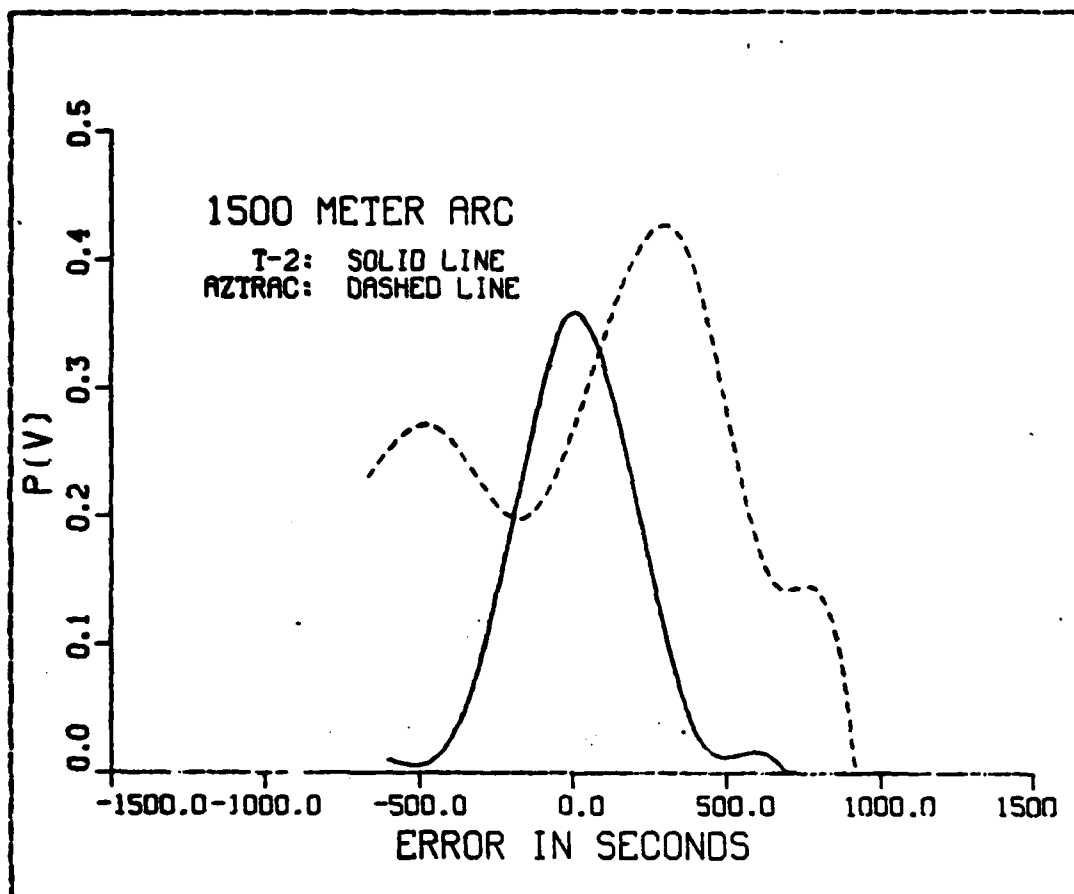


Figure C.5 Probability Density Plot: 1500 m arc.

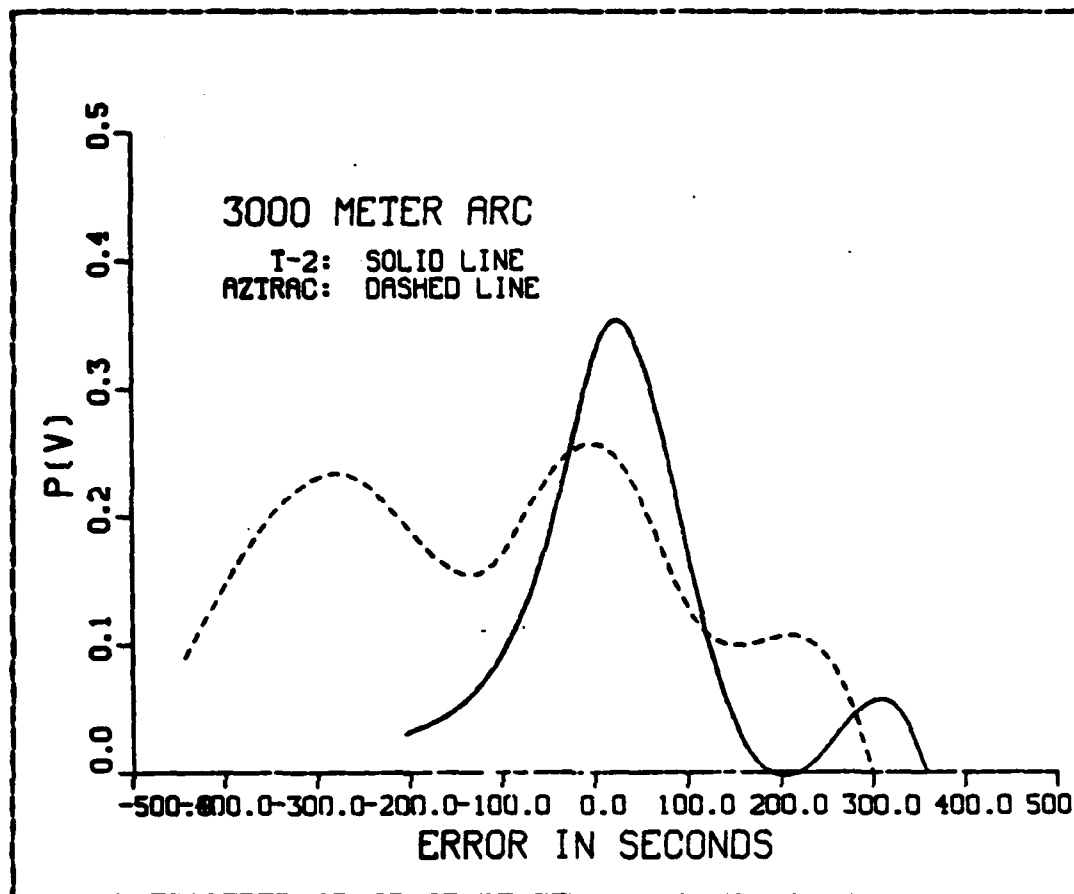


Figure C.6 Probability Density Plot: 3000 m arc.

## BIBLIOGRAPHY

- Apsey, B., private communication, Jion Offshore Surveys, Inc., Baton Rouge, LA, 1983.
- Bowditch, N., American Practical Navigator, Defense Mapping Agency Hydrographic Center, 1977.
- Box, G., Hunter, W. G., and Hunter, J. S., Statistics for Experimenters, John Wiley and Sons, 1978.
- Burt, W. A., and others, Mathematical Considerations Pertaining to the Accuracy of Position Location and Navigation Systems, Part I, Naval Warfare Research Center Research Memorandum, NWRM-RM34, Stanford Research Institute, Menlo Park, CA., 1966.
- Crow, E. L., Davis, F. A., and Maxfield, M. W., Statistics Manual, U.S. Naval Ordnance Test Station China Lake, 1955.
- Davis, R. E., and others, Surveying Theory and Practice, McGraw-Hill, 1981.
- Ehrhardt, J. E., FORTTRAN subroutine TCARC, NOAA Atlantic Marine Center, Norfolk, VA, 1979.
- Greenwalt, C. R., and Shultz, M. E., Principles of Error Theory and Cartographic Applications, ACIC Technical Report NO. 96, USAF Aeronautical Chart and Information Center, St. Louis., MO, 1962.
- Greenwalt, C. R., User's Guide to Understanding Chart and Geodetic Accuracies, ACIC Reference publication no. 28, USAF Aeronautical Chart and Information Center, St. Louis, MO, 1971.
- Hart, D. E., private communication, US Army Corps of Engineers Waterways Experiment Station, Vicksburg, MI, July, 1983.
- Hart, D. E., and Downing, G.C., Positioning Techniques and Equipment for US Army Corps of Engineers Hydrographic Surveys, Technical Report H-77-15, US Army Engineer Waterways Experiment Station, Vicksburg, MI, May, 1977.
- Heinzen, H. R., Hydrographic Surveys: Geodetic Control Criteria, M. S. thesis, Cornell University, 1977.
- Null, C., and Nie, N., SPSS Update 7-9, McGraw-Hill, 1981.

Ingham, A. E., Hydrography for the Surveyor and Engineer, Granada, 1974.

International Hydrographic Organization, Accuracy Standards Recommended for Hydrographic Surveys, SP 44, 1968.

International Hydrographic Organization, Accuracy Standards Recommended for Hydrographic Surveys, SP 44, 1982.

Kaplan, A., Error Analysis of Hydrographic Positioning and the Application of Least Squares, M. S. Thesis, Naval Postgraduate School, Monterey, 1980.

Mueller, I. I., Spherical and Practical Astronomy as applied to Geodesy, Frederick Ungar Publishing Co., New York, 1969.

Munson, R. C., Positioning Systems: Report on the Work of WG414b, paper presented at the XV International Congress of Surveyors, Stockholm, Sweden, 1977.

Newell, V. E., and Winter, D., Application of the Global Positioning System to Nearshore Hydrographic Surveys, M. S. Thesis, Naval Postgraduate School, Monterey, 1981.

Odon Offshore Surveys, Inc., Aztrac System Technical Manual, 1982.

Palikaris, A. E., Methods of Hydrographic Surveying used in Different Countries, M. S. Thesis, Naval Postgraduate School, Monterey, 1983.

Pfeifer, L. J., FORTTRAN subroutine INVER1, NOAA National Ocean Service, Rockville, MD, 1975.

Pfeifer, L. J., FORTTRAN subroutine DIRECT1, NOAA National Ocean Service, Rockville, MD, 1975.

Robinson, D. W., FORTTRAN subroutine HISTG, Naval Postgraduate School, Monterey, CA, 1974.

Silva, C., Calculation of Hydrographic Position Data by Least Squares Adjustment, M. S. Thesis, Naval Postgraduate School, Monterey, 1979.

Smith, J. G., A New High Precision Range/Azimuth Position Fixing System, Sea Technology, V.24, pp. 33-36, March, 1983.

Thomson, D. B., and Wells, D. E., Hydrographic Surveying I, Lecture Notes No. 45, Department of Surveying Engineering, University of New Brunswick, Canada, 1977.



Umbach, M. J., Hydrographic Manual Fourth Edition, NOAA  
National Ocean Service, 1976.

Wallace, J. L., Hydroplot/Hydrolog System Manual, National  
Ocean Service Technical Manual No. 2, 1977.

Wallace, J. L., private communication, NOAA National Ocean  
Service, Rockville, MD, September, 1983.

Walpole, R. E., and Meyers, R. H., Probability and  
Statistics for Engineers and Scientists, Macmillan, 1978.

Wonnacott, T. H., and Wonnacott, R. W., Introductory  
Statistics, John Wiley and Sons, 1977.

# INITIAL DISTRIBUTION LIST

	No. Copies
1. Defense Technical Information Center Cameron Station Alexandria, VA 22314	2
2. Library, Code 0142 Naval Postgraduate School Monterey, CA 93943	2
3. Chairman (Code 63Mr) Department of Oceanography Naval Postgraduate School Monterey, CA 93943	1
4. LCDR Gerald B. Mills, NOAA (Code 68mi) Department of Oceanography Naval Postgraduate School Monterey, CA 93943	1
5. Cdr Donald E. Puccini, USN Fleet Numerical Oceanography Center Monterey, CA 93940	1
6. Director Naval Oceanography Division Naval Observatory 34th and Massachusetts Avenue NW Washington, D.C. 20390	1
7. Commander Naval Oceanography Command Bay St. Louis, MS 39522	1
8. Commanding Officer Naval Oceanographic Office NSTL Station Bay St. Louis, MS 39522	1
9. Commanding Officer Naval Ocean Research and Development Activity NSTL Station Bay St. Louis, MS 39522	1
10. Chairman, Oceanography Department U. S. Naval Academy Annapolis, MD 21402	1
11. Chief of Naval Research 800 N. Quincy Street Arlington, VA 22217	1
12. Director (Code PPH) Defense Mapping Agency Bldg. 56, U. S. Naval Observatory Washington, D.C. 20305	1

13. Director (Code HO)  
Defense Mapping Agency Hydrographic  
Topographic Center  
6500 Brookes Lane  
Washington, D.C. 20315 1
14. Director (Code PSD-MC)  
Defense Mapping School  
Ft. Belvoir, VA 22060 1
15. Director, Charting and Geodetic Services (N/CG)  
National Oceanic and Atmospheric Administration  
Rockville, MD 20852 1
16. Chief, Program Planning, Liaison,  
and Training (NC2)  
National Oceanic and Atmospheric Administration  
Rockville, MD 20852 1
17. Chief, Nautical Charting Division (N/CG2)  
National Oceanic and Atmospheric Administration  
Rockville, MD 20852 1
18. Chief, Hydrographic Surveys Branch (N/CG24)  
National Oceanic and Atmospheric Administration  
Rockville, MD 20852 1
19. Director, Pacific Marine Center (N/HOP)  
National Ocean Service, NOAA  
1801 Fairview Avenue East  
Seattle, WA 98102 1
20. Director, Atlantic Marine Center (N/HOA)  
National Ocean Service, NOAA  
439 W. York Street  
Norfolk, VA 23510 1
21. Commanding Officer  
NOAA Ship RAINIER  
Pacific Marine Center, NOAA  
1801 Fairview Avenue East  
Seattle, WA 98102 1
22. Commanding Officer  
NOAA Ship FAIRWEATHER  
Pacific Marine Center, NOAA  
1801 Fairview Avenue East  
Seattle, WA 98102 1
23. Commanding Officer  
NOAA Ship DAVIDSON  
Pacific Marine Center, NOAA  
1801 Fairview Avenue East  
Seattle, WA 98102 1
24. Commanding Officer  
NOAA Ship HT. MITCHELL  
Atlantic Marine Center, NOAA  
439 West York Street  
Norfolk, VA 23510 1
25. Commanding Officer  
NOAA Ship WHITING  
Atlantic Marine Center, NOAA  
439 West York Street  
Norfolk, VA 23510 1

26. Commanding Officer 1  
NOAA Ship P. M. RICE  
Atlantic Marine Center, NOAA  
439 West York Street  
Norfolk, VA 23510
27. Chief, Hydrographic Field Parties Section 1  
NOA 233  
Atlantic Marine Center, NOAA  
439 West York Street  
Norfolk, VA 23510
28. Maureen R. Kenny, LT, NOAA 1  
N/HOP 21x2  
7600 Sand Point Way NE  
Bin C15700 Bldg. 3  
Seattle, WA 98115-0070
29. LT David A. Waltz, NOAA 1  
1475 Spring Meadow Lane  
Suffolk, VA 23432
30. LT Christine W. Schomaker, NOAA 1  
NOAA/NGDC E/GC3  
325 Broadway  
Boulder, CO 80303
31. IHO/FIG International Advisory Board 1  
International Hydrographic Bureau  
Avenue President J. F. Kennedy  
Monte Carlo, Monaco
32. LT Athanasios E. Palikaris 1  
72 Timotheou Street  
Athens TR512  
Greece
33. Mr. Dunny Green 1  
SMC 2780 NPS  
Monterey, CA 93943
34. LCDR Lisa Williams, Venezuelan Navy 1  
SMC 1070 NPS  
Monterey, CA 93943
35. Ing. Walter Herrera 1  
Instituto Nacional de Canalizaciones  
Zona Industrial de la Ferrominera  
Puerto Ordaz  
Estado Bolívar  
Venezuela

LMED  
-8